Dynamics of the reaction-diffusion system $A + B \to 0$ with input of particles

Boris M. Shipilevsky
Institute of Solid State Physics, Chernogolovka, Moscow district, 142432, Russia
(February 1, 2008)

We study dynamics of filling of an initially empty finite medium by diffusing particles A and B, which arise on the surface upon dissociation of AB molecules, impinging on it with a fixed flux density I, and desorb from it by the reaction $A+B \to AB \to 0$. We show that once the bulk diffusivities differ ($p = D_A/D_B < 1$), there exists a critical flux density $I_c(p)$, above which the relaxation dynamics to the steady state is qualitatively changed: on time dependences of c_{As}/c_e (c_e being the steady state concentration at $t \to \infty$) a maximum appears, the amplitude of which grows both with I and with D_B/D_A ratio. In the diffusion-controlled limit $I \gg I_c$ at $p \ll 1$ the reaction "selects" the *universal laws* for the particles number growth $\mathcal{N}_A = \mathcal{N}_B \propto t^{1/4}$ and the evolution of the surface concentrations $c_{As} \propto t^{-1/4}, c_{Bs} \propto t^{1/4}$, which are approached by one of the *two characteristic regimes* i) and ii) with the corresponding hierarhy of the intermediate power-law asymptotics. In the first of these c_{As} goes through a comparatively *sharp* $\max(c_{As}/c_e) \propto I^{1/6}$, the amplitude of which is p-independent, in the second one c_{As} goes through a *plateau-like* $\max(c_{As}/c_e) \propto p^{-1/4}$, the amplitude of which is I-independent. We demonstrate that on the main filling stage the evolution of the $\mathcal{N}(t)/\mathcal{N}_e, c_{As}(t)/c_e$, and $c_{Bs}(t)/c_e$ trajectories with changing p or J between the limiting regimes i) and ii) is unambigouosly defined by the value of the scaling parameter $\mathcal{K} = p^{3/2}J$ (J being the reduced flux density) and is described by the set of *scaling laws*, which we study in detail analytically and numerically. In conclusion, we analyze specific features of the long-time relaxation dynamics and calculate exactly the relaxation rate $\omega(p, J)$.

82.20Mj, 05.70 Ln

I. INTRODUCTION

For the last decade the reaction-diffusion system $A + B \to 0$, where unlike species A and B diffuse and irreversibly react in the bulk of a d-dimensional substrate, has acquired the status of one of the most popular objects in nonequilibrium statistical physics [1]. Two situations have been investigated most intensively: (i) dynamics of the $A + B \to 0$ annihilation in an infinite system with initially homogeneously (randomly) and equimolarly distributed reactants, in which below the critical dimension $d_c = 4$ a dynamical clustering develops (fluctuation-induced like-particle domains formation) and, as a result, an anomalous reaction deceleration arises (Ovchinnikov and Zeldovich, 1978 [2], Toussaint and Wilczek, 1983 [3]); (ii) behaviour of the dynamic reaction front in an infinite system with initially spatially separated reactants (Galfi and Racz, 1988 [4]), and structure of the steady state front in a finite system, at the ends of which are injected equal currents of $A's$ and $B's$ particles (Ben-Naim and Redner, 1992 [5], Cornell and Droz, 1993 [6]).

Recently, we have shown [7,8], that in another wide class of RD system, where reaction and diffusion are spatially separated (i.e. reaction proceeds on the surface of the medium and diffusion proceeds in its bulk) the interplay between reaction and diffusion acquires qualitatively new features and leads to the threshold self-organizing dynamics of the $A+B \to 0$. It has been found that once particles A and B diffuse at different mobilities from the bulk of finite medium onto the surface and die on it by the reaction $A + B \to 0$, there should exist some threshold difference in the initial numbers of A and B particles , Δ_c, above which the process of their death , instead of usual deceleration, starts *to accelerate autocatalytically*. Moreover, it has been demonstrated [9] that in the diffusion-controlled limit $\Delta \to \infty$ a new critical phenomenon develops in the system - *annihilation catastrophe*, which arises as a result of self-organizing explosive growth (drop) of the surface concentrations of, respectively, slow and fast particles (*concentration explosion*) and manifests itself in the form of an abrupt singular jump in the desorption flux relaxation rate. In the limit of strong difference of diffusivities the annihilation catastrophe leads to the phenomenon of abrupt disappearance of the flux (*flux breaking effect*), which may pretend to be one of the most dramatic manifestations of the reaction-diffusion interplay.

The aim of this paper is, in contrast to the pure annihilation problem $A+B \to 0$, to consider dynamics of filling of an *initially empty* finite medium by diffusing particles A and B, which arise on the surface upon dissociation of AB molecules, impinging on it with a *fixed* flux density I, and desorb from it by the reaction $A+B \to AB \to 0$. We assume that the density of the input flux I is not too large and (or) the reaction rate constant is sufficiently large so that in the process of filling up to the steady state the surface coverages by adatoms A_{ads} and B_{ads} remain small enough and, therefore, the reflection of AB molecules from the occupied sites can be neglected. In addition, we assume that the particles exchange rates between the surface and the subsurface layer are great, and already at early stages of diffusion into the bulk a quasiequilibrium

is reached between the surface and the subsurface layer. Finally, we assume that in our $2d$-reaction + $3d$-diffusion problem diffusion smoothes out lateral fluctuations and, hence, planar distribution of $A's$ and $B's$ particles is sustained mesoscopically uniform, so that 1) the desorption flux density may be described by the mean-field expression and 2) the problem can effectively be considered as one dimensional. In the framework of these assumptions we formulate a closed system of nonlinear boundary value diffusion problems, which we then investigate in detail analytically and numerically.

II. MODEL

Let the both surfaces $X = \pm\ell$ of an initially empty infinitely extended slab of thickness 2ℓ be hit with a fixed-density I flux of AB molecules, which dissociate on unoccupied sites to adatoms A_{ads} and B_{ads} with probability 1. Adatoms A_{ads} and B_{ads} migrate along the surface and either, on running into one another, irreversibly desorb by the reaction $A_{ads} + B_{ads} \rightarrow AB \rightarrow 0$ or diffuse into the bulk, gradually filling it to some steady state concentration $c_e(I)$ (Fig.1). Because of planar spatial homogeneity (see below), the bulk diffusion flux must be directed normally to the surface plane, that is, the problem is effectiveliy one dimensional. The boundary conditions for the bulk diffusion equations

$$\partial_t c_i = D_i \partial_X^2 c_i \tag{1}$$

$(i = A, B)$ can be derived from the balance of the flux densities on the surface

$$\dot{\rho_i} = I^a - I^d - I_i^{sb} \tag{2}$$

and in the subsurface layer

$$a\dot{c}_{is} = I_i^{sb} - I_i^D \mid_s . \tag{3}$$

Here ρ_i is the surface concentration of i-adatoms (cm^{-2}), $c_{is} = c_i \mid_{X=\ell}$ is the concentration of i-particles in the subsurface layer (cm^{-3}), a is the lattice parameter, I^a and I^d are adsorption and desorption flux densities, $I_i^{sb} = \mathcal{I}_i^s - \mathcal{I}_i^b = \Gamma_i^s \rho_i - \Gamma_i^b c_{is}\theta_0$ is the surface-to-subsurface layer flux density, where Γ_i^s and Γ_i^b are the rate constants of i- particles transition from the surface into the subsurface layer and back, respectively, $\theta_0 = 1 - \theta_A - \theta_B$ is the fraction of vacant sites on the surface, which we take to be close to unity ($\theta_i \ll 1$), $I_i^D \mid_s = D_i \partial_X c_i \mid_{X=\ell}$ is the diffusion flux density at the surface (by symmetry, we consider the interval $[0, \ell]$ only with the condition $\partial_X c_i \mid_{X=0} = 0$). We assume that the subsurface layer - surface barrier is not much different from the diffusion barrier in the bulk ($\Gamma_i^b \sim D_i/a$), and probability of the adatoms transition to the subsurface layer is much greater than probability of their desorption ($\mathcal{I}_i^s \gg I^d$). Then, prior to desorbing, the particles multiply go to the subsurface layer and back, and already at early stages of diffusion into the bulk a quasiequilibrium must be established between the surface and the subsurface layer, $\rho_i \simeq f_i c_{is}$, where $f_i = \Gamma_i^b/\Gamma_i^s$ is the surface segregation coefficient. Moreover, if the surface segregation is not enough strong (at elevated temperatures usually $f \sim (1 - 10^2)a$), and the system size is quite large, $\ell \gg f_i$, then at comparatively short (in ℓ^2/D_i scale) times $f_i \ll \ell_i^D = \sqrt{D_i t} \ll \ell$, when the number of particles in the bulk (per surface unit) $\mathcal{N}_i = \int_0^\ell c_i dX \sim c_{is}\sqrt{D_i t}$ much exceeds that on the surface $f_i c_{is}$, the capacities of the subsurface layer ($I_i^D \mid_s = I_i^{sb}$) and of the surface ($f_i|\dot{c_{is}}| \ll I_i^D \mid_s$) may be neglected, therefore conditions (2) and (3) are degenerated to the following

$$\dot{\mathcal{N}}_i = I_i^D \mid_s = I^a - I^d.$$

According to Refs. [10], [11], and [12], in a distributed d- dimensional system $A + B \rightarrow 0$ with injection of A and B particles, with their difference being strictly conserved (correlated landing), a critical (marginal) dimensionality, above which no fluctuation-induced segregation of A and B occurs, equals $d_c = 2$ ($2d$-reaction + $2d$-diffusion). It is to be expected that in our case ($2d$-reaction + $3d$-diffusion) $3d$-diffusion smoothes out lateral fluctuations, and a planar distribution of A and B particles is sustained mesoscopically uniform. So, the desorption flux density may be described by the mean-field expression $I^d = k\rho_A\rho_B$. From the condition $I_i^{sb} = I^a - I^d$ it follows

$$\rho_i = f_i c_{is}\theta_0[1 + (I^a - I^d)/\mathcal{I}_i^b],$$

therefore, taking $I^a - I^d \ll \mathcal{I}_i^b$, we obtain

$$I^d = \kappa c_{As} c_{Bs}\theta_0^2[1 + (I^a - I^d)(1/\mathcal{I}_A^b + 1/\mathcal{I}_B^b)],$$

where $\kappa = k f_A f_B$ is the effective reaction rate constant (cm^4/s). The above requirement $I^a, I^d \ll \mathcal{I}_i^s \simeq \mathcal{I}_i^b$ imposes on the concentrations limitations $I^a/\Gamma_A^b \ll c_{As} \ll \Gamma_B^b/\kappa, I^a/\Gamma_B^b \ll c_{Bs} \ll \Gamma_A^b/\kappa$, the lower boundary of which defines the conditions for the crossover to the subsurface layer-surface quasiequilibrium regime. Restrictions on the flux densities $I^d, I^a \ll \Gamma_A^b\Gamma_B^b/\kappa$ follow herefrom. Taking into account the reflection from occupied sites, we write $I^a = I\theta_0^2$ to obtain $I^a - I^d = \chi\theta_0^2(I - \kappa c_{As}c_{Bs})$, where factor $\chi = [1 + \theta_0((\kappa/\Gamma_B^b)c_{As} + (\kappa/\Gamma_A^b)c_{Bs})]^{-1} \simeq 1$. So, after a short-term transient stage $t \gg t_{tr} = \max(f_i^2/D_i)$ the boundary conditions take the form

$$\dot{\mathcal{N}}_i = D_i \partial_X c_i \mid_s = \chi\theta_0^2(I - \kappa c_{As}c_{Bs}), \tag{4}$$

where $1 - \chi\theta_0^2 \ll 1$. We assume that on a transient stage the desorption can be neglected, i.e. $t_{tr} \ll t_q$, where t_q is a characteristic time at which the desorption flux becomes comparable with the input flux $I^d \sim I$. Using then the Laplace transform, at $t \ll t_q, t_i^D = \ell^2/D_i$ one can easily obtain the complete solution of (1)-(3),

wherefrom at $t \gg t_{if} \gg t_{is}$ (here $t_{is} = D_i/(\Gamma_i^b)^2$ and $t_{if} = f_i^2/D_i$) it follows

$$\mathcal{N}_i = \mathcal{N}_i^{(0)} \left[1 - \frac{2}{\sqrt{\pi}} \left(\frac{t_{if}}{t}\right)^{1/2} + \cdots\right],$$

$$c_{is} = c_{is}^{(0)} \left[1 - \frac{\sqrt{\pi}}{2} \left(\frac{t_{if}}{t}\right)^{1/2} + \cdots\right], \qquad (5)$$

$$\rho_i = f_i c_{is} \left[1 + \frac{\sqrt{\pi}}{2} \left(\frac{t_{is}}{t}\right)^{1/2} + \cdots\right],$$

where $\mathcal{N}_i^{(0)} = It$ and $c_{is}^{(0)} = \frac{2I\sqrt{t}}{\sqrt{\pi D_i}}$ are the solutions of (1),(4) with the initial conditions $c_i(X,0) = 0$ at $\chi\theta_0^2 = 1$ and $I^d/I \to 0$. From (5) it is seen that the influence of the transient stage rapidly decays in time. So, as we are mainly interested here in the system's behavior at $t \gg t_{tr}$, we shall take $c_i(X,0) = 0$ as the initial condition for (1), (4). According to (5), the condition $I^d \sim \kappa I^2 t/\sqrt{D_A D_B} \ll I$ is reduced to the requirement $t \ll t_q = \frac{\sqrt{D_A D_B}}{I\kappa}$, whence it follows $I \ll \sqrt{D_A D_B}/\kappa t_{tr}$. Introducing the index "H" (*heavy*) for the slower diffusing species and the index "L" (*light*) for the faster one, taking $\chi\theta_0^2 = 1$ and going to dimensionless variables, we come finally to the boundary value diffusion problem

$$\partial h/\partial\tau = \nabla^2 h \quad , \quad \partial l/\partial\tau = (1/p)\nabla^2 l, \qquad (6a)$$

$$\nabla h \mid_s = (1/p)\nabla l \mid_s = J - h_s l_s, \qquad (6b)$$

with the conditions of symmetry $\nabla(h,l) \mid_{x=0} = 0$ and the initial conditions $h(x,0) = l(x,0) = 0$. Here $h(x,\tau) = c_H/c_*$ and $l(x,\tau) = c_L/c_*$ are the reduced concentrations, $J = I/I_*$ is the reduced flux density, $\nabla =\equiv \partial/\partial x$ $x = X/\ell \in [0,1]$ is the nondimensional coordinate, $\tau = D_H t/\ell^2$ is the nondimensional time, $p = D_H/D_L \leq 1$ is the ratio of species diffusivities, $I_* = \kappa c_*^2 = (D_H/\sqrt{k}\ell)^2$ and $c_* = D_H/\kappa\ell$ are the characteristic flux density and concentration scales, from which the relaxation dynamics to the steady-state becomes diffusion-controlled (in the reaction-controlled regime the both species are distributed uniformly $c_{is} = \mathcal{N}/\ell = It/\ell$, so, from the condition $I^d \sim \kappa(It/\ell)^2 \ll I$ it follows $t_R \sim \ell/\sqrt{\kappa I}$. By comparing t_R with the characteristic diffusion time of heavy species $t_i^D \sim \ell^2/D_H$, we obtain $I_* = (D_H/\sqrt{\kappa}\ell)^2$).

According to (5), with an accuracy to a neglibly small capacity of the surface layer ($\tau \gg \tau_{tr} = \max(d_H^2, pd_L^2)$, $d_i = f_i/\ell \ll 1$), equal amounts (per surface unit) of H and L particles diffuse into the bulk $\mathcal{N}_H = \mathcal{N}_L = \mathcal{N}$, therefore in the steady state ($\tau \to \infty$)

$$h_e = l_e = N_e = \sqrt{J},$$

where $N = \mathcal{N}/\mathcal{N}_*$ is the reduced number of particles and $\mathcal{N}_* = c_*\ell = D_H/\kappa$ is the characteristic scale of the number of particles. In dimensionless variables requirement $1 - \chi \ll 1$ with account of $\Gamma_i^b \sim D_i/a$ leads to the conditions $h_s \ll \Gamma_L^b \ell/D_H \sim p^{-1}(\ell/a)$ and $l_s \ll \Gamma_H^b \ell/D_H \sim \ell/a$ whence there follows a limitation on the reduced flux density $l_e = h_e = \sqrt{J} \ll \ell/a$ and, therefore, $J \ll J_\chi^u \sim (\ell/a)^2$. The requirement $\theta_i \sim a^2\rho_i \ll 1$ leads to the conditions $h_s \ll (\kappa/a^2 D_H)d_H^{-1}$ and $l_s \ll (\kappa/a^2 D_H)d_L^{-1}$, whence by assuming $d_H \sim d_L$ we obtain $J \ll J_\theta^u \sim (\kappa/a^2 D_H)^2 d_H^{-2}$. Finally, the requirement $\tau_{tr} \ll \tau_q = 1/J\sqrt{p}$ leads to the condition $J \ll J_{tr}^u \sim d_H^{-2}/\sqrt{p}$. In macroscopic systems the quantities J_χ^u and J_{tr}^u are very large (for example at $\ell \simeq 10^{-1} cm$ and $f_H \sim f_L \sim 10a$ we have $J_\chi^u \sim 10^{14}$ and $J_{tr}^u \sim 10^{12}/\sqrt{p}$). At temperatures of intensive desorption ($\kappa/a^2 D_H \geq 1$) the quantity J_θ^u is as large. So, the reduced flux density J can, formally, be taken as being unlimitedly variable.

III. TRANSITION IN RELAXATION DYNAMICS

At a high enough density of the input flux, J, a quasiequilibrium $J^d = h_s l_s \simeq J$ should be established well before the particles distribution in the bulk becomes uniform. In view of the fact that at $p < 1$ there must be $l_s < h_s$, this means $h_s/h_e > 1$, i.e. at sufficiently large J the H particles surface concentration should initially grow to some maximum $h_s^M > h_e$ and then, as a result of diffusion into the bulk, relax asymtotically to its steady state value, h_e, from above. We thus conclude that at $p < 1$ there ought to exist a critical flux density $J_c(p)$, above which the relaxation character is qualitatively changed. In this section we give a *linear* analysis of the long-time relaxation dynamics, in terms of which we find the relaxation rate $\omega(J,p)$ and the exact value of $J_c(p)$.

We introduce the new variables $\tilde{h} = h_e - h, \tilde{l} = l_e - l$ and $\tilde{n} = N_e - N$. Then, instead of (6) we have

$$\partial\tilde{h}/\partial\tau = \nabla^2\tilde{h}, \quad \partial\tilde{l}/\partial\tau = (1/p)\nabla^2\tilde{l}, \qquad (7a)$$

$$\nabla\tilde{h} \mid_s = (1/p)\nabla\tilde{l} \mid_s = -\sqrt{J}(\tilde{h}_s + \tilde{l}_s) + \tilde{h}_s\tilde{l}_s \qquad (7b)$$

with $\nabla(\tilde{h},\tilde{l}) \mid_{x=0} = 0$. In a long-time limit $\tilde{h},\tilde{l} \mid_{\tau\to\infty} \to 0$ the nonlinear term may be neglected, so by satisfying (7), we find the leading terms of the long-time relaxation in the form

$$\tilde{h} = \mathcal{A}_H \cos(\sqrt{\omega}x)e^{-\omega\tau}, \quad \tilde{l} = \mathcal{A}_L \cos(\sqrt{p\omega}x)e^{-\omega\tau}, \qquad (8)$$

where $\mathcal{A}_L = (\sqrt{p}\sin\sqrt{\omega}/\sin\sqrt{p\omega})\mathcal{A}_H$, and the relaxation rate $\omega(p,J)$ is defined by the least positive root of the equation

$$\cot\sqrt{\omega} = \sqrt{\frac{\omega}{J}} - \sqrt{p}\cot\sqrt{p\omega} \qquad (9)$$

It follows from (8) that long-time asymptotics of surface concentrations as a function of the particles number $\tilde{n} = \int_0^1 \tilde{h}dx = \int_0^1 \tilde{l}dx$ has the form

$$\tilde{h}_s \mid_{\tilde{n}\to 0} = (\sqrt{\omega}\cot\sqrt{\omega})\tilde{n}, \tilde{l}_s \mid_{\tilde{n}\to 0} = (\sqrt{p\omega}\cot\sqrt{p\omega})\tilde{n}, \quad (10)$$

whence

$$r_s = \frac{\tilde{h}_s}{\tilde{l}_s} \mid_{\tilde{n}\to 0} = \frac{\cot\sqrt{\omega}}{\sqrt{p}\cot\sqrt{p\omega}} = -1 + \sqrt{\frac{\omega}{Jp}}\tan(\sqrt{p\omega}). \quad (11)$$

According to (9), with growing J the relaxation rate is increased from $\omega = 2\sqrt{J}$ in the reaction-controlled limit $\sqrt{J} \ll 1$

$$\omega = 2\sqrt{J}(1 - \frac{1+p}{3}\sqrt{J} + \cdots), \quad \sqrt{J} \ll 1$$

to a maximal

$$\omega = \omega_m(p)(1 - b(p)/\sqrt{J} + \cdots), \quad \sqrt{J} \gg 1$$

in the diffusion-controlled limit $\sqrt{J} \gg 1$, the maximal relaxation rate $\omega_m(p)$ growing herewith from

$$\omega_m(1) = \pi^2/4$$

at $p \to 1$ to

$$\omega_m(0) = 4.1158...$$

at $p \to 0$ ($b(p)$ changes from $b(1) = 1$ to $b(0) = 1.348...$). So, in accord with (9),(10), we conclude that at $p < 1$ there exists a critical relaxation rate $\omega_c = \pi^2/4$, which is reached at a critical flux density

$$J_c = \frac{\pi^2}{4p}\tan^2(\pi\sqrt{p}/2), \qquad (12)$$

above which the quantity $\tilde{h}_s$ reverses its sign ($+ \to -$), i.e. the character of the surface concentration relaxation of H particles qualitatively changes: at $J < J_c$ the h_s value grows to h_e monotonously, whereas at $J > J_c$ the value of h_s reaches initially a maximum and then relaxes to h_e from above (Fig.2). According to (11), as J grows, the ratio $r_s = \tilde{h}_s/\tilde{l}_s \mid_{n\to 0}$ is changed from 1 at $\sqrt{J/J_c} \ll 1$

$$r_s = 1 - \frac{2}{3}\sqrt{J}(1-p) + \cdots, \quad \sqrt{J/J_c} \ll 1$$

to -1 at $\sqrt{J/J_c} \gg 1$

$$r_s = -1 + \sqrt{\frac{\omega_m}{Jp}}\tan\sqrt{p\omega_m}, \quad \sqrt{J/J_c} \gg 1$$

as is illustrated for $p = 0.1$ in Figs.3 and 4, the first of which demonstrates the dependences of r_s on J/J_c, calculated from (9), (11), the second one demonstrates the time dependences of h_s/h_e and l_s/l_e at $J = J_c$ and $J = 10^3$, numerically calculated from (6).

Eqs. (10) and (11) carry no information on the initial conditions, so they, clearly, remain valid at any initial number of particles $\mathcal{N}_H(0) = \mathcal{N}_L(0) = \mathcal{N}(0)$ and at their arbitrary initial distribution. In this case, according to (11), if the initial distribution is uniform, and $\tilde{n} > 0$, i.e. the initial particles number is less than the steady state one, then at $J > J_c$ the h_s value passes a maximum and relaxes to the steady state level *from above*, whereas if the initial distribution is uniform, and $\tilde{n} < 0$, i.e. the initial particles number is greater than the steady state one, then at $J > J_c$ the h_s value passes a mimimum and relaxes to the steady state level *from below*.

In the present paper the main attention will be focused on the behavior of the surface concentrations and the growth dynamics of the particles number in the diffusion-controlled limit $J \gg J_c$, which is of greatest interest. As at $\omega\tau > 1$ deviations from the steady state become exponentially small then, clearly, in the diffusion-controlled limit the main nonlinear kinetic effects evolve in times $\tau \ll 1$ when the diffusion of H particles proceeds, actually, into a semi-infinite medium. In the next Section we shall consider the dynamics of behavior of h_s,l_s and N at $\tau \ll 1$, taking into account the reflection from the boundary $x = 0$, and then, in Section V, we shall come back to an analysis of the long-time relaxation and obtain expressions for the $\mathcal{A}_i(J,p)$ amplitudes.

IV. DIFFUSION OF H PARTICLES INTO A SEMI-INFINITE MEDIUM ($\tau \ll 1$).

By applying the Laplace transform $\hat{f}(s) = \hat{\mathcal{L}}f(\tau) = \int_0^\infty e^{-s\tau}f(\tau)d\tau$ to Eqs. (6), one can easily obtain a formal solution of problem (6) in the form

$$\hat{h}(x,s) = \hat{h}_s\frac{\cosh(x\sqrt{s})}{\cosh\sqrt{s}}, \quad \hat{l}(x,s) = \hat{l}_s\frac{\cosh(x\sqrt{sp})}{\cosh\sqrt{sp}} \quad (13)$$

with the boundary conditions (6b), which can, for convenience, be represented as

$$\hat{N} = \frac{\hat{h}_s}{\sqrt{s}}\tanh\sqrt{s} = \frac{\hat{l}_s}{\sqrt{sp}}\tanh\sqrt{sp} \qquad (14)$$

and

$$\hat{N} = \frac{J}{s^2} - s^{-1}\hat{\mathcal{L}}(h_s l_s). \qquad (15)$$

The system of equations (14) and (15) comletely defines the behavior of $N(\tau), h_s(\tau)$, and $l_s(\tau)$ which, in turn, define the evolution of spatial particles distribution via Eqs.(13). In the limit of our interest here $\tau \ll 1$ the first of Eqs.(14) is reduced to

$$\hat{N} = \frac{\hat{h}_s}{\sqrt{s}}(1 - 2e^{-2\sqrt{s}} + \cdots), \qquad (16)$$

where in expansion of $\tanh\sqrt{s}$ in power-series of $e^{-2\sqrt{s}}$ the leading term $O(e^{-1/\tau})$, which takes into account the contribution of reflection from the boundary $x = 0$, is retained. The second characteristic time $\tau_L = p$, at which the diffusive length L of particles becomes equal to the system's size, separates two temporal regions, $\tau \ll p$ and $\tau \gg p$, within which the growth dynamics of the particles number is qualitatively different. Within $\tau \ll p$ the L particles duffusion proceeds, actually, into a semi-infinite medium, and from (14) we have

$$\hat{N} = \frac{\hat{l}_s}{\sqrt{sp}}(1 - 2e^{-2\sqrt{sp}} + \cdots). \tag{17}$$

In the opposite limit, $\tau \gg p$, the L particles distribution becomes practically uniform, and from (14) it follows

$$\hat{N} = \hat{l}_s\left(1 - \frac{1}{3}sp + \cdots\right), \tag{18}$$

where in expansion of $\tanh\sqrt{sp}$ in power-series of $\sqrt{sp}$ the leading term $O(p/\tau)$ is retained, which in the case of the power growth $l_s \propto \tau^n$ leads to the law

$$N = l_s\left[1 - \frac{n}{3}\left(\frac{p}{\tau}\right) + \cdots\right]. \tag{19}$$

In what follows, we shall consider the dynamics of crossover from the adsorption-controlled regime to the diffusion-controlled one first in the limit of $\tau \ll p$, when H and L particles diffuse into a semi-infinite medium, then in the limit $p \ll \tau \ll 1$, when H particles diffuse into a semi-infinite medium at a uniform L particles distribution.

A. Diffusion of H and L particles into a semi-infinite medium ($\tau \ll p$).

On neglecting the reflection from the boundary $x = 0$, we have from (16) and (17)

$$\hat{h}_s = \frac{\hat{l}_s}{\sqrt{p}} = \hat{N}\sqrt{s}. \tag{20}$$

The system of equations (15) and (20) is reduced to the nonlinear integral equation that cannot be solved in the general form. Our aim will be, starting with (20), to obtain asymptotics for the solution of (15)-(17) in the limits of $J^D\mid_s \simeq J \gg J^d$ (adsorption-controlled regime) and $J^d \simeq J \gg J^D\mid_s$ (diffusion-controlled regime).

1. Adsorption-controlled regime ($\tau \ll p, \tau_q$)

By assuming $N = J\tau$, i.e. by neglecting the contribution of desorption, from (20) we obtain

$$h_s = l_s/\sqrt{p} = (2/\sqrt{\pi})J\sqrt{\tau},$$

whence it follows that the adsorption-controlled asymptotics has the form

$$h_s = \frac{2}{\sqrt{\pi}}J\sqrt{\tau}(1 + \varrho_H),$$

$$l_s = \frac{2}{\sqrt{\pi}}J\sqrt{\tau p}(1 + \varrho_L), \tag{21}$$

$$N = J\tau(1 + \varrho_N),$$

where $\varrho_i \ll 1$. Thus, the condition of smallness of desorption flux is $J^d = h_s l_s = (4/\pi)J^2\sqrt{p}\tau \ll J$, whence it follows that it takes place at $\tau \ll \tau_q = 1/J\sqrt{p}$. Substituting the expression for J^d into (15), we obtain $N = J\tau(1 - \frac{2}{\pi}(\tau/\tau_q) + \cdots)$. Substituting further this expression into (16) and (17), with an accuracy to the leading terms, we finally obtain

$$\varrho_H = -\frac{8}{3\pi}\left(\frac{\tau}{\tau_q}\right) + 2\sqrt{\pi}ierfc\frac{1}{\sqrt{\tau}} + \cdots,$$

$$\varrho_L = -\frac{8}{3\pi}\left(\frac{\tau}{\tau_q}\right) + 2\sqrt{\pi}ierfc\sqrt{\frac{p}{\tau}} + \cdots, \tag{22}$$

$$\varrho_N = -\frac{2}{\pi}\left(\frac{\tau}{\tau_q}\right) + \cdots,$$

where the function $ierfc(\eta) = e^{-\eta^2}/\sqrt{\pi} - \eta erf(\eta)$ at $\eta \gg 1$ has the asymptotic form $e^{-\eta^2}(1 - 3/2\eta^2 + \cdots)/2\sqrt{\pi}\eta^2$.

2. Diffusion-controlled regime ($\tau_q \ll \tau \ll p$).

In this limit, by neglecting the contribution of the transient region, i.e. by assuming $\tau_q \to 0$, from (20) and (15) we have

$$h_s = l_s/\sqrt{p}, \quad h_s l_s = J,$$

whence we find $h_s = h_e p^{-1/4}, l_s = l_e p^{1/4}$ and, subsequently, according to (20), we obtain $N = 2\sqrt{J/\pi}p^{-1/4}\sqrt{\tau}$ and, hence, $J^D\mid_s = J(\frac{\tau_q}{\tau})^{1/2}/\sqrt{\pi}$. Thus, the diffusion-controlled asymptotics has the form

$$h_s = h_e p^{-1/4}(1 + \lambda_H),$$

$$l_s = l_e p^{1/4}(1 + \lambda_L), \tag{23}$$

$$N = \frac{2}{\sqrt{\pi}}N_e p^{-1/4}\sqrt{\tau}(1 + \lambda_N),$$

where $\lambda_i \ll 1$. Substituting (23) into Eqs. (15), (16), and (17), we find that, asymptotically, λ_H and λ_L are connected by relationships

$$\lambda_H - \lambda_L = -2\left(erfc\sqrt{\frac{p}{\tau}} - erfc\frac{1}{\sqrt{\tau}}\right) + \cdots,$$

$$\lambda_H + \lambda_L = -\frac{1}{\sqrt{\pi}}\left(\frac{\tau_q}{\tau}\right)^{1/2} + \cdots,$$

whence, with taking account of (16) and (17), we finally obtain

$$\lambda_H = -\frac{1}{2\sqrt{\pi}}\left(\frac{\tau_q}{\tau}\right)^{1/2} - erfc\sqrt{\frac{p}{\tau}} + erfc\frac{1}{\sqrt{\tau}},$$

$$\lambda_L = -\frac{1}{2\sqrt{\pi}}\left(\frac{\tau_q}{\tau}\right)^{1/2} + erfc\sqrt{\frac{p}{\tau}} - erfc\frac{1}{\sqrt{\tau}}, \qquad (24)$$

$$\lambda_N = -\frac{\sqrt{\pi}}{4}\left(\frac{\tau_q}{\tau}\right)^{1/2} - \sqrt{\pi}\left(ierfc\sqrt{\frac{p}{\tau}} + ierfc\frac{1}{\sqrt{\tau}}\right),$$

where comlementar error function $erfc(\eta) = 1 - erf(\eta)$ at $\eta \ll 1$ has the asymptotics $e^{-\eta^2}(1 - 1/2\eta^2 + \cdots)/\sqrt{\pi}\eta$.

B. Diffusion of H particles into a semi-infinite medium at uniform distribution of L particles ($p \ll \tau \ll 1$).

By neglecting the H particles reflection from the boundary $x = 0$ and nonuniformity of the distribution of L particles, from (16) and (18) we have

$$\hat{N} = \hat{l}_s = \hat{h}_s/\sqrt{s}. \qquad (25)$$

Evidently, the character of the crossover onto regime (25) depends on the τ_q/τ_L relation. In the region of $\tau_q \ll \tau_L$ regime (25) is realized after a quasiequilibrium $h_s l_s \simeq J$ has been reached, whereas in the opposite limit, $\tau_L \ll \tau_q$, the crossover to regime (25) occurs directly at the initial stage when the desorption can yet be neglected.

1. Adsorption-controlled regime ($p \ll \tau \ll \tau_*$).

By assuming $N = J\tau$, i.e. by neglecting the contribution of desorption, from (25) we have

$$N = l_s = J\tau, \quad h_s = (2/\sqrt{\pi})J\sqrt{\tau}, \qquad (26)$$

whence it follows that the adsorption-controlled asymptotics has the form

$$h_s = \frac{2}{\sqrt{\pi}}J\sqrt{\tau}(1 + \Delta_H),$$

$$l_s = J\tau(1 + \Delta_L), \qquad (27)$$

$$N = J\tau(1 + \Delta_N).$$

According to (26), the condition of smallness of the desorption flux takes now the form $J^d = h_s l_s \simeq (2/\sqrt{\pi})J^2\tau^{3/2} \ll J$, whence it follows that it is realized at times $\tau \ll \tau_* = J^{-2/3}$. So, under the conditions of uniform distribution of L particles, there appears a new characteristic time scale $\tau_* = J^{-2/3}$ in the vicinity of which the crossover from the adsorption-controlled to the diffusion-controlled regime occurs. Using the exact series expansion in particular points

$$\coth\sqrt{sp} = \frac{1}{\sqrt{sp}} + 2\sum_{n=1}^{\infty}\frac{\sqrt{sp}}{sp + (\pi n)^2},$$

we find from (14)

$$\hat{l}_s = \hat{N}\left\{1 + \frac{1}{3}sp - 2\sum_{n=1}^{\infty}\frac{(sp/\pi n)^2}{sp + (\pi n)^2}\right\}, \qquad (28)$$

and, therefore, in the limit $\tau/\tau_* \to 0$ we have exactly

$$l_s = J\tau\left\{1 + \frac{1}{3}\left(\frac{p}{\tau}\right)\left[1 - \frac{6}{\pi^2}\sum_{n=1}^{\infty}n^{-2}e^{-\frac{(\pi n)^2\tau}{p}}\right]\right\},$$

whence it is seen that the addition to (19) becomes negligibly small $O(e^{-\pi^2})$ already at $\tau \sim p$. Substituting the expression for J^d into (15), we obtain $N = J\tau(1 - \frac{4}{5\sqrt{\pi}}(\frac{\tau}{\tau_*})^{3/2} + \cdots)$. Substituting then this expression into (16) and (28), respectively, we finally find

$$\Delta_H = -\frac{3\sqrt{\pi}}{8}\left(\frac{\tau}{\tau_*}\right)^{3/2} + 2\sqrt{\pi}ierfc\frac{1}{\sqrt{\tau}} + \cdots,$$

$$\Delta_L = \frac{1}{3}\left(\frac{p}{\tau}\right) - \frac{4}{5\sqrt{\pi}}\left(\frac{\tau}{\tau_*}\right)^{3/2} + \cdots, \qquad (29)$$

$$\Delta_N = -\frac{4}{5\sqrt{\pi}}\left(\frac{\tau}{\tau_*}\right)^{3/2} + \cdots.$$

2. Diffusion-controlled regime ($p, \tau_* \ll \tau \ll 1$)

By neglecting the contribution of the transient region, i.e. by taking $p, \tau_* \to 0$ and assuming that h_s changes by the power law $h_s \sim \tau^n$, from (25) and (15) we have

$$N = l_s = \gamma(n)h_s\sqrt{\tau}, \quad h_s l_s = J, \qquad (30)$$

where $\gamma(n) = \Gamma(n+1)/\Gamma(n+3/2)$ and $\Gamma(n)$ is the gamma function. From (30) it immediately follows $n =$

$-1/4$. Thus, the exact asymptotic solution of (15),(25) in the limit $p \to 0, J \to \infty$ is

$$N = l_s = l_e \beta \tau^{1/4}, \quad h_s = h_e \beta^{-1} \tau^{-1/4}, \tag{31}$$

where $\beta = [\Gamma(3/4)/\Gamma(5/4)]^{1/2} = 1.1627366....$ With account taken of the contribution of the transient region and reflection of H particles from the boundary $x = 0$, we, finally, obtain the diffusion-controlled asymptotics in the form

$$h_s = h_e \beta^{-1} \tau^{-1/4}(1 + \phi_H),$$

$$l_s = l_e \beta \tau^{1/4}(1 + \phi_L), \tag{32}$$

$$N = N_e \beta \tau^{1/4}(1 + \phi_N).$$

Substituting (32) into (15) and (18) and taking $\phi_i \ll 1$ we find that, asymptotically, ϕ_H, ϕ_L, and ϕ_N are connected by the relationships

$$\phi_H + \phi_L = -\frac{\beta}{4}\left(\frac{\tau_*}{\tau}\right)^{3/4} + \cdots \tag{33}$$

and

$$\phi_N = \phi_L - \frac{1}{12}\left(\frac{p}{\tau}\right) + \cdots. \tag{34}$$

Substituting then (32) into Eq.(16), we come to the equation

$$\beta^2 \hat{\mathcal{L}}(\phi_N \tau^{1/4}) = s^{-1/2} \hat{\mathcal{L}}(\phi_H/\tau^{1/4}) - \frac{2\Gamma(3/4)}{s^{5/4}} e^{-2\sqrt{s}}, \tag{35}$$

which, on neglecting the contribution of H particles reflection from the boundary $x = 0$, takes the form

$$\beta^2 \hat{\mathcal{L}}(\tilde{\phi}_N \tau^{1/4}) = s^{-1/2} \hat{\mathcal{L}}(\tilde{\phi}_H/\tau^{1/4}). \tag{36}$$

Assuming that $\tilde{\phi}_i$ decay asymptotically in time by the power-law

$$\tilde{\phi}_i = \mathcal{C}_i/\tau^{\nu_i} + \cdots, \tag{37}$$

where $\mathcal{C}_i(p, \tau_*) \to 0$ as $p, \tau_* \to 0$, from (33),(34) and (36) it can easily be shown that the exponents $\nu_i \geq 3/4$. Indeed, let $\nu_H < 3/4$. Then, from (36) it follows that $\nu_L = \nu_H$, and the coefficients $\mathcal{C}_L$ and $\mathcal{C}_H$ have like signs, which contradicts the condition (33). Thus, $\nu_i \geq 3/4$ which suggests that in contrast to the diffusion-controlled asymptotics (23), the sign and value of the $\mathcal{C}_L$ and $\mathcal{C}_H$ are governed by all the prehistory of transition to the asymptotics (31) and can be calculated only numerically. In the next sections we shall discuss the behavior of $\tilde{\phi}_L$ and $\tilde{\phi}_H$ in more detail and demonstrate that it is quite nontrivial. We now consider the contribution into ϕ_i due to the reflection of H particles from the boundary $x = 0$. According to (33) and (34), in the limit $p, \tau_* \to 0$ we have

$$\phi_H = -\phi_L = -\phi_N = \phi^{(0)}.$$

Substituting $\phi^{(0)}$ into Eq.(35), we obtain

$$\beta^2 \hat{\mathcal{L}}(\phi^{(0)} \tau^{1/4}) = \frac{2\Gamma(3/4)}{s^{5/4}} e^{-2\sqrt{s}} - s^{-1/2} \hat{\mathcal{L}}(\phi^{(0)}/\tau^{1/4}). \tag{38}$$

It is easy to check that the inverse Laplace transform of the solution of Eq.(38) ought to have the form

$$\phi^{(0)} = \frac{2\Gamma(5/4)}{\sqrt{\pi}} \tau^{3/4} e^{-1/\tau}(1 + g), \tag{39}$$

where

$$g = c_{1/2}\tau^{1/2} + c_1 \tau + c_{3/2}\tau^{3/2} + \cdots.$$

Substituting Eq.(39) into (38) and equlizing the coefficients at the same s powers, we finally find

$$c_{1/2} = -\frac{1}{\beta^2}, c_1 = -\frac{15}{16} + \frac{1}{\beta^4}, c_{3/2} = \frac{1 - c_1}{\beta^2}.$$

C. Two characteristic paths of the crossover to the diffusion-controlled regime with uniform L particle distribution.

According to subsections A) and B), depending on the relation of three characteristic times $\tau_L = p, \tau_q$, and τ_*, the crossover to the diffusion-controlled regime with uniform L particles distribution proceeds by one of the two qualitatively different scenarios. One of these is realized in the limit $\tau_q \ll p \ll 1$, when at first, a quasiequilibrium between the input and desorption fluxes is established in the system (crossover $A1 \to A2$ at $\tau \sim \tau_q$), following which the L particles distribution becoms uniform (crossover $A2 \to B2$ at $\tau \sim p$). In this case, the surface concentrations h_s, l_s and particle number N go, respectively, through the following chains of power-law asymptotics:

$$h_s: \quad \tau^{1/2} \to \tau^0 \to \tau^{-1/4},$$

$$l_s: \quad \tau^{1/2} \to \tau^0 \to \tau^{1/4}, \tag{40}$$

$$N: \quad \tau^1 \to \tau^{1/2} \to \tau^{1/4}.$$

The second scenario is realized in the limit $p \ll \tau^* \ll 1$, when at first the L particles distribution becomes uniform (crossover $A1 \to B1$ at $\tau \sim p$), whereupon a quasiequilibrium is established between the input and desorption fluxes (crossover $B1 \to B2$ at $\tau \sim \tau_*$). In this case, h_s, l_s, and N go, respectively, through the following chains of power-law asymptotics:

$$h_s: \quad \tau^{1/2} \to \tau^{-1/4},$$

$$l_s: \quad \tau^{1/2} \to \tau^1 \to \tau^{1/4}, \tag{41}$$

$$N: \quad \tau^1 \to \tau^{1/4}.$$

It can easily be shown from Eqs.(13) that at each of the given power-law asymptotics, $h_s \propto \tau^n, \tau \ll 1$, the spatial distribution of H-particles changes, on neglecting the contribution of the transient regions, by the law

$$h(x,\tau) = h_s \mathcal{F}_n\left(\frac{1-x}{2\sqrt{\tau}}\right), \tag{42}$$

where

$$\mathcal{F}_n(\xi) = \begin{cases} \pi^{1/2} i erfc(\xi), & n = 1/2 \\ erfc(\xi), & n = 0 \\ \frac{2^{1/4}\Gamma(3/4)}{\sqrt{\pi}} e^{-\xi^2/2} \mathcal{D}_{-1/2}(\sqrt{2}\xi), & n = -1/4. \end{cases}$$

Here $\mathcal{D}_\nu(z)$ is the function of parabolic cylinder which at $z \gg 1$ has the asymptotics $\mathcal{D}_\nu(z) = e^{-z^2/4} z^\nu [1 - \nu(\nu-1)/2z^2 + \ldots]$. The spatial distribution of L particles at asymptotics $l_s \propto \tau^n, \tau \ll p$ with $n = 1/2, 0$ has exactly the same form, except for the substitution $\tau \to \tau/p$.

By comparing the paired ratios of the characteristic times τ_L, τ_q, and τ_*, we find

$$\frac{\tau_L}{\tau_q} = \left(\frac{\tau_L}{\tau_*}\right)^{3/2} = \left(\frac{\tau_*}{\tau_q}\right)^3 = \mathcal{K} = p^{3/2} J, \tag{43}$$

whence it is seen that the character of the system's evolution is governed by the value of the parameter $\mathcal{K} = p^{3/2}J$: at any p and J relation in the limit $\mathcal{K} \gg 1$ the system evolves in accord with the chains of asymptotics (40), whereas in the opposite limit, $\mathcal{K} \ll 1$, the system evolves in accord with the chains of asymptotics (41). On neglecting the reflection of H particles from the boundary $x = 0$, one can easily see that in the limit $\mathcal{K} \to \infty (\tau_q/p \to 0)$ the only characteristic time scale is defined by the quantity p, therefore, as suggested by (23) and (32), the behavior of h_s and l_s should have the scaling form

$$h_s/h_e = p^{-1/4} w_H(\tau/p), \quad l_s/l_e = p^{1/4} w_L(\tau/p), \tag{44}$$

where the scaling functions $w_i(\zeta)$ have asymptotics $w_{H,L}(\zeta) = 1 \mp erfc(1/\sqrt{\zeta})$ at $\zeta \ll 1$ and $w_{H,L}(\zeta) \simeq (\beta\zeta^{1/4})^{\mp 1}$ at $\zeta \gg 1$. Indeed, substituting (44) into (14) and (15) and going to the Lasplace transform with respect to the reduced time $\zeta = \tau/p \to s$, in the limit $\mathcal{K} \to \infty$ we find

$$w_H w_L = 1, \quad \hat{w}_H = \hat{w}_L \tanh\sqrt{s},$$

whence it immediately follows $w_i = w_i(\tau/p)$ and, hence, $\tilde{\phi}_i = \tilde{\phi}_i(\tau/p)$. In the opposite limit, $\mathcal{K} \to 0 (p/\tau_* \to 0)$, the only characteristic time scale is defind by the quantity τ_*, therefore, in accord with (27) and (32), the behavior of h_s and l_s should have the scaling form

$$h_s/h_e = J^{1/6} v_H(\tau/\tau_*), \quad l_s/l_e = J^{-1/6} v_L(\tau/\tau_*), \tag{45}$$

where the scaling functions $v_i(\zeta)$ have asymptotics $v_H(\zeta) \simeq 2\sqrt{\zeta/\pi}, v_L(\zeta) \simeq \zeta$ at $\zeta \ll 1$ and $v_{H,L} \simeq (\beta\zeta^{1/4})^{\mp 1}$ at $\zeta \gg 1$. Indeed, substituting (45) into (14) and (15) and going to the Laplace transform with respect to the reduced time $\zeta = \tau/\tau_* \to s$, in the limit $\mathcal{K} \to 0$ we find

$$\hat{\mathcal{L}}(v_H v_L) = s^{-1}(1 - s^2 \hat{v}_L), \quad \hat{v}_H = \hat{v}_L \sqrt{s},$$

whence it immediately follows $v_i = v_i(\tau/\tau_*)$ and, hence, $\tilde{\phi}_i = \tilde{\phi}_i(\tau/\tau_*)$.

From (45) it follows that in the limit $\mathcal{K} \to 0$ the crossover to the diffusion-controlled regime is characterized by a comparatively sharp maximum of h_s/h_e, the height of which depends solely on J and changes with growing J by the law

$$h_s^M/h_e = b_H J^{1/6}. \tag{46}$$

In the opposite limit $\mathcal{K} \to \infty$, according to (23),(44), a maximum of h_s/h_e is degenerated to an extended plateau, of which the height depends on p alone

$$h_s^M/h_e = p^{-1/4}, \tag{47}$$

and the extension, defined as the ratio of the times, which bound the region $\lambda_H \le \epsilon \ll 1$, grows with J as $\propto \mathcal{K}\epsilon^2/\ln(1/\epsilon)$.

In the next subsections we give the results of a detailed numerical study of the dynamics of the system in question, enabling one to gain a complete picture of evolution of h_s, l_s, and N "trajectories" between two limiting regimes (40) and (41).

D. Numerical calculations

The numerical integration of equations (6) was performed by means of the *implicit* discretization scheme of increased accuracy with an additional *"fictitious"* node at the surface. The scheme allowed performing the calculations in the system with strong difference in species diffusivities with an accuracy down to $10^{-3}\%$ (see below). The space and time steps were changed within the ranges $\delta x \simeq 3\times10^{-4} \div 3\times10^{-6}$ and $\delta\tau \simeq 10^{-4} \div 10^{-11}$, respectively, with the number of time steps being $10^5 \div 10^6$. The evolution dynamics of $h_s(\tau), l_s(\tau)$, and $N(\tau)$ was studied in the ranges of $p = 10^{-10} \div 1$ and $J = 10^{-1} \div 10^{12}$.

1. Kinetic diagrams $p - J - \tau$

Fig.5(a) illustrates the time dependences $h_s(\tau)/h_e, l_s(\tau)/l_e$, and $N(\tau)/N_e$,

calculated numerically at a fixed flux density $J = 10^8$ for p values ranging from 1 to 10^{-9} (the arrows show the directions of shift of the corresponding trajectories at a change of p from $p = 1$ (bold curves) to $p = 10^{-9}$ (bold curves)). One can clearly see the whole set of power-law asymptotic regions (40),(41) of h_s, l_s, and N trajectories and the character of their evolution as p (and, hence, $\mathcal{K}$) are decreased from the values corresponding to the limiting regime (40) ($p \gg 5 \times 10^{-6}, \mathcal{K} \gg 1$) to those of (41) ($p \ll 5 \times 10^{-6}, \mathcal{K} \ll 1$) where the dependences of the trajectories on p dissapears and they asymptotically approach those shown in bold lines. In accord with (46) and (47), as p decreases, the plateau on the curves $h_s(\tau)/h_e$ is transformed to a comparatively sharp maximum, the height of which depends only on J. At all $p \ll 1$ the $h_s/h_e, l_s/l_e$, and N/N_e trajectories come to the universal asymptotics $(\beta\tau^{1/4})^{\mp 1}$ (31). Herewith, as seen from Fig.5a and will be demonstrated in detail in what follows, the $h_s(\tau)/h_e$ trajectories always come to the asymptotics $(\beta\tau^{1/4})^{-1}$ only *from above*, whereas the $l_s(\tau)/l_e$ trajectories always come to the asymptotics $\beta\tau^{1/4}$ only *from below*.

By defining the boundaries of the asymptotic regions so that within their confines the condition

$$\max\{|\delta_a|, |d\delta_a/d\ln\tau|\} \leq 0.01 \tag{48}$$

shall hold (here $\delta_a \equiv \{\varrho_i, \lambda_i, \Delta_i, \phi_i, \sigma_i\}, \sigma_i$ describes the exponential relaxation to the steady state according to Eqs.(69)), we have carried out an extensive numerical study of the positions of the corresponding boundaries for $J = 10^8$ and p values, ranging from 1 to 10^{-10} (we have calculated and analyzed trajectories for 100 values of p, 10 for each order). Figs.5b and c show the kinetic $p - \tau$ diagrams of the regions of the power-law asymptotics and steady state (shaded by light gray) for the $h_s(\tau)/h_e$ and $l_s(\tau)/l_e$ trajectories, respectively. In Fig.5c by dark gray is distinguished the $\beta\tau^{1/4}$ asymptotic region for the $N(\tau)/N_e$ trajectories of the growth of the particles number. From Figs.5b,c it is seen that the dashed lines of the characteristic times $\tau_q, \tau_*, \tau_L = p$ and $\tau_H = 1$ divide the $p - \tau$ plane into several segments, confining the regions of the power-law asymptotics τ^n with $n = 1/2, 0, 1$ and $\mp 1/4$. The boundaries of these regions go in parallel with the lines of the corresponding characteristic times, in accord with Eqs. (22), (24), (29), (39), (44) and (45). The τ_q, τ_L, and τ_* lines intersect in the point $\mathcal{K} = 1$ ($\tau_q = \tau_L = \tau_* = 4.64158 \times 10^{-6}$), shown by filled circle, in accord with Eq.(43). As the $n = 1/2, 0, 1$ region boundary positions are described by Eqs. (22), (24) and (26), we shall focus mainly on the $n = \mp 1/4$ region boundary positions.

From Figs.5b,c it is seen that, in accord with (44), at $p \gg 5 \times 10^{-6} (\mathcal{K} \gg 1)$ the left-hand boundaries of the $n = \mp 1/4$ regions go in parallel with the τ_L line down to the point of intersection of left- and right-hand boundaries of $n = 0$ regions ($p \approx 2 \times 10^{-3}, \mathcal{K} \approx 5 \times 10^3$) where the plateau on the h_s and l_s trajectories disappears. Above this point the h_s/h_e and l_s/l_e approarch the $(\beta\tau^{1/4})^{\mp 1}$ asymptotics *simultaneously* and, which is important, this occurs at $\tau \approx p$, i.e. *long before* the L particles distribution in the bulk becomes uniform (left boundary of the $n = 1/4$ region shaded by dark gray in Fig.5c). Such synhchronization of the trajectories directly follows from Eqs.(33) and (44), according to which in the scaling limit $\mathcal{K} \to \infty$ ($\tau_*/p \to 0$) $w_H w_L = 1$ and $\phi_H = -\phi_L$. In the opposite limit $p \ll 5 \times 10^{-6} (\mathcal{K} \ll 1)$ the left boundaries of $n = \mp 1/4$ regions become parallel to the τ_* line in the vicinity of the intersection point of $n = 1/2$ boundary (Fig.5b) with the τ_L line ($p \approx 3 \times 10^{-7}, \mathcal{K} \approx 2 \times 10^{-2}$), in accord with Eq.(45). Below this point (i) the behavior of $h_s(\tau)$ obeys the scaling law (45), i.e. it ceases to be dependent on p and (ii) the boundaries of $n = 1/4$ regions of growth of $l_s(\tau)$ and $N(\tau)$ merge, i.e. by the instant of the transition to asymptotics $\beta\tau^{1/4}$ the distribution of L particles becomes *uniform*. Essentially, that in this region of p and $\mathcal{K}$ the behavior of h_s and l_s becomes strongly *asymmetric*: the transition of the h_s/h_e trajectories to $(\beta\tau^{1/4})^{-1}$ asymptotics takes place *well before* the l_s/l_e trajectories reach the $\beta\tau^{1/4}$ asymptotics. Below the point $p \approx 2 \times 10^{-9}, \mathcal{K} \approx 10^{-5}$, where on the kinetic diagram of Fig.5c there appears the $n = 1$ region, the merging of the $l_s(\tau)$ and $N(\tau)$ trajectories takes place already on the stage of the adsorption-controlled regime, beyond which the $l_s(\tau)$ trajectory ceases to be p-independent.

With account taken of the fact that the boundaries of the asymptotic regions are strongly related to the characteristic times τ_L, τ_q, and τ_*, one can easily get from Fig.5b,c the idea of how the kinetic diagrams evolve with changing density of the input flux J. Indeed, as J grows, the point $\mathcal{K} = 1$ should shift along the τ_L line, as shown by arrows in Fig.5b,c, entailing the τ_q and τ_* lines. The τ_q and τ_* lines, shifting in parallel to themselves, should in turn entail the lines of the corresponding boundaries of the asymptotic regions, so that with growing J the $n = 0, \mp 1/4$ regions should expand in a self-similar manner, and the $n = 1/2, 1$ regions contract in a self-similar manner. From the conditions $\tau_{-1/4} \simeq \tau_r$ and $\tau_{1/4} \simeq \tau_r$, where $\tau_{-1/4} = 5.855\tau_*$ and $\tau_{1/4} = 93.88\tau_*$ are the positions of the left boundaries of regions $n = -1/4$ and $n = 1/4$ at $\mathcal{K} \to 0$ and $\tau_r \approx 0.2$ is the position of their right boundary associated with the influence of the H particles reflection from the boundary $x = 0$, one can conclude that the starting flux densities for the appearance of $\tau^{-1/4}$ and $\tau^{1/4}$ asymptotics are $J_{-1/4} \approx 10^2$ and $J_{1/4} \approx 10^4$, respectively. From Fig.5b,c it follows that the vertices of $n = \mp 1/4$ regions for the surface concentrations and the number of particles are in the points $p_s \approx 0.1$ and $p_N \approx 2 \times 10^{-2}$, respectively. Thus, the $J - p$ limits of $(\beta\tau^{1/4})^{\mp 1}$ asymptotics are defined by the following conditions:

$$h_s : p < p_s \approx 0.1, J > J_{-1/4} \approx 10^2,$$

$$l_s : p < p_s \approx 0.1, J > J_{1/4} \approx 10^4,$$

$$N : p < p_N \approx 2 \times 10^{-2}, J > J_{1/4} \approx 10^4.$$

2. Maximum of h_s

Figs.6a and b illustrates the behavior of the maximum of the surface H particles concentration, h_s^M/h_e,(a) and the time for which this maximum is reached, τ_M,(b) as a function of growing J. The curves are calculated numerically at fixed $p = 10^{-1}, 10^{-2}, 10^{-3}, 10^{-4}, 10^{-5}$ and 10^{-6}. It is seen that, in accord with (45),(46), at small $\mathcal{K} \ll 1$ the calculated curves approach the p-independent power-law asymptotics (shown in the dashed lines)

$$h_s^M/h_e = 0.7221 J^{1/6}, \quad \tau_M = 1.125 J^{-2/3}. \tag{49}$$

As J grows, the dependences of h_s^M/h_e and τ_M on J deviate from the p-independent asymptotics (49) the earlier the large is p, reaching at $\mathcal{K} \gg 1$ the J-independent plateau (47) (as seen for the curves for $p = 10^{-1}$ and $p = 10^{-2}$). Interestingly that at $p \ll 1$ the curves approach the power-law asymptotics (49) already at comparatively small flux densities $J \approx 50$, exceeding J_c by no more than an order of magnitude.

3. Behavior of ϕ_H and ϕ_L

We shall now consider the regularities of the behavior of transient terms $\phi_H(\tau)$ and $\phi_L(\tau)$, which characrerize the kinetics of the transition of surface concentrations to the universal asymptotics $(\beta\tau^{1/4})^{\mp 1}$. Fig.7 shows the dependences $\phi_H(\tau)$(a) and $\phi_L(\tau)$(b), calculated numerically at $p = 10^{-4}$ for J values, ranging from $J = 10^4$ to $J = 10^{12}$ (from $\mathcal{K} = 10^{-2}$ to $\mathcal{K} = 10^6$, respectively). It is seen that (i) the ϕ_H value at any $\mathcal{K}$ first crosses zero, changing the sign from - to + , then reaches a maximum and asymptotically approaches zero only *from above*; (ii) the ϕ_L value at any $\mathcal{K}$ asymptotically approaches zero only *from below*, in this case, with $\mathcal{K} < 1$ it occurs monotonously whereas with $\mathcal{K} \gg 1$ the ϕ_L value first crosses zero, changing the sign from + to - , then reaches in modulus a maximum, and only after this begins to approach zero; (iii) with a growth in J the ϕ_H maximum is shifted left and its amplitude grows, whereas the $|\phi_L|$ maximum is shifted right and its amplitude drops, so that at $\mathcal{K} > 10^6$ the behavior of $\phi_H(\tau)$ and $\phi_L(\tau)$ becomes comletely "symmetric", in agreeement with (33), (44)

$$\phi_H(\tau) = |\phi_L(\tau)|.$$

From Fig.8 where are presented the sections of the dependences $\phi_H(\tau) > 0$(a) and $\phi_L(\tau) < 0$(b) replotted in double logarithmic coordinates, we find that at $J \gg J_{1/4}$ the ϕ_H and ϕ_L values decrease at a sufficient distance from the ϕ_H maximum by the power law (37) with the exponents $\nu_H = \nu_L = 3/4$

$$\tilde{\phi}_i = \mathcal{C}_i/\tau^{3/4} + \cdots \tag{50}$$

up to $\tau \approx 0.1 \div 0.2$ where a rapid growth of $|\phi_i|$ begins due to the reflection of H particles from the boundary $x = 0$. At the growth stage the $|\phi_i|$ dependences are seen to go exactly onto the bold $\phi^{(0)}$ curve, calculated from Eq.(39). It is important to note that from Fig.8 it directly follows that the error of numerical calculations does not exceed $\approx 10^{-3}$%. According to Eq.(44) in the scaling limit $\mathcal{K} \to \infty$ from (50) and (33) it follows

$$\tilde{\phi}_i = m_i^\infty (p/\tau)^{3/4} + \cdots,$$

where the coefficients $m_H^\infty = -m_L^\infty$ are independent of J and p. From the data of Fig.8 we find at $\mathcal{K} > 10^6$

$$m_H^\infty = -m_L^\infty = 0.023 \tag{51}$$

and obtain for the maximum $|\phi_i|^m$ and the time of its attaining τ_i^m

$$\phi_H^m = |\phi_L|^m = 0.00798, \quad \tau_i^m = 2.51p. \tag{52}$$

In Fig.9 are plotted in double logarithmic coordinates the sections of the dependences $\phi_H(\tau) > 0$(a) and $\phi_L(\tau) < 0$(b), calculated numerically at a fixed flux density $J = 10^6$ for the p values, ranging from $p = 10^{-2}$ to $p = 10^{-6}$ (from $\mathcal{K} = 10^3$ to $\mathcal{K} = 10^{-3}$, respectively). The both maxima, ϕ_H^M and $|\phi_L|^M$, are seen to shift towards smaller τ with decreasing p, herewith the ϕ_H maximum amplitude decreases, whereas the $|\phi_L|$ maximum amplitude increases, and at $\mathcal{K} < 1$ it disappears. At $p \ll p_s$ the $\phi_H(\tau)$ and $\phi_L(\tau)$ dependences decay at a distance from ϕ_H^m by the power law (50), converging to the p independent trajectories at $p \approx 10^{-6} (\mathcal{K} \approx 10^{-3})$. According to Eq.(45) in the scaling limit $\mathcal{K} \to 0$ from (50) and (33) it follows

$$\tilde{\phi}_i = m_i^0 (\tau_*/\tau)^{3/4} + \cdots,$$

where the p- and J-independent coefficients m_i^0 should satisfy the condition

$$m_H^0 + m_L^0 = -\beta/4 = -0.29068.... \tag{53}$$

From the data of Fig.9, in accord with (53), we find at $\mathcal{K} < 10^{-3}$

$$m_H^0 = 0.014, \quad m_L^0 = -0.305 \tag{54}$$

and obtain for the ϕ_H^m maximum and the time of its attaining τ_H^m

$$\phi_H^m = 0.00108, \quad \tau_H^m = 17.3\tau_*. \tag{55}$$

E. Scaling and universality

So far the main attention has been focused on the limiting regimes $\mathcal{K} \ll 1$ and $\mathcal{K} \gg 1$ and on specific features of the crossover between these regimes at a change in J for p =const. or at a change in p for J =const. We shall now show that at $\tau \ll 1$, when the H particles reflection from the boundary $x = 0$ can be neglected, the behavior of h_s, l_s, and N is described by the scaling laws

$$h_s = h_e p^{-1/4} W_H(\mathcal{K}, T),$$

$$l_s = l_e p^{1/4} W_L(\mathcal{K}, T), \tag{56}$$

$$N = N_e p^{1/4} W_N(\mathcal{K}, T),$$

where $T = \tau/p$ and the scaling functions $W_i(\mathcal{K}, T)$ depend on the only parameter $\mathcal{K} = p^{3/2}J$. Indeed, going to the Laplace transform with respect to the reduced time $T \to s$, on substituting (56) into Eqs.(14) and (15) and neglecting the terms, related to the H particles reflection from the boundary $x = 0$, we easily find

$$\hat{W}_N = \frac{\hat{W}_H}{\sqrt{s}} = \frac{\hat{W}_L}{\sqrt{s}} \tanh\sqrt{s}, \tag{57}$$

$$\hat{W}_N = \frac{\sqrt{\mathcal{K}}}{s^2}(1 - s\hat{\mathcal{L}}(W_H W_L)), \tag{58}$$

whence it follows $W_i = W_i(\mathcal{K}, T)$. In agreement with the results of Sections IVA and B, the asymptotic behavior of the scaling functions $W_i(\mathcal{K}, T)$ on the power-law portions of the h_s, l_s, and N trajectories have the following form:

A) Diffusion of H and L particles into a semi-infinite medium ($T \ll 1$).

1. Adsorption-controlled regime ($T \ll 1, 1/\mathcal{K}$).

$$W_H = \frac{2}{\sqrt{\pi}}\sqrt{\mathcal{K}T}\left(1 - \frac{8}{3\pi}\mathcal{K}T + \cdots\right),$$

$$W_L = \frac{2}{\sqrt{\pi}}\sqrt{\mathcal{K}T}\left(1 - \frac{8}{3\pi}\mathcal{K}T + Te^{-1/T} + \cdots\right), \tag{59}$$

$$W_N = T\sqrt{\mathcal{K}}\left(1 - \frac{2}{\pi}\mathcal{K}T + \cdots\right).$$

2. Diffusion-controlled regime ($1/\mathcal{K} \ll T \ll 1$).

$$W_{H,L} = 1 - \frac{1}{2\sqrt{\pi\mathcal{K}T}} \mp erfc\frac{1}{\sqrt{T}} + \cdots, \tag{60}$$

$$W_N = 2\sqrt{T/\pi}\left(1 - \tfrac{1}{4}\sqrt{\frac{\pi}{\mathcal{K}T}} - \sqrt{\pi}ierfc\frac{1}{\sqrt{T}} + \cdots\right).$$

B) Diffusion of H particles into a semi-infinite medium at uniform distribution of L particles ($1 \ll T \ll 1/p$).

1. Adsorption-controlled regime ($1 \ll T \ll 1/\mathcal{K}^{2/3}$).

$$W_H = \frac{2}{\sqrt{\pi}}\sqrt{\mathcal{K}T}\left(1 - \frac{3\sqrt{\pi}}{8}\mathcal{K}T^{3/2} + \cdots\right),$$

$$W_L = T\sqrt{\mathcal{K}}\left(1 + \frac{1}{3T} - \frac{3\sqrt{\pi}}{8}\mathcal{K}T^{3/2} + \cdots\right), \tag{61}$$

$$W_N = T\sqrt{\mathcal{K}}\left(1 - \frac{4}{5\sqrt{\pi}}\mathcal{K}T^{3/2} + \cdots\right).$$

2. Diffusion-controlled regime ($T \gg 1, 1/\mathcal{K}^{2/3}$).

$$W_{H,L} = (\beta T^{1/4})^{\mp 1}(1 + m_{H,L}(\mathcal{K})T^{-3/4} + \cdots), \tag{62}$$

$$W_N = \beta T^{1/4}\left(1 - \frac{1}{12T} + m_L(\mathcal{K})T^{-3/4} + \cdots\right).$$

According to Eqs.(56), at arbitrary changes in J and p, with $\mathcal{K}$ =const. retained, the scaling functions are the *universal* functions of the reduced time, $W_i(T)$, and the $h_s/h_e, l_s/l_e$, and N/N_e trajectories are shifted by a factor

$$p^{\mp 1/4} = (J/\mathcal{K})^{\pm 1/6}.$$

So, the boundaries of the power-law asymptotic regions, the W_H and $|\phi_i|$ maxima, the times at which they are attained, T_M and T_i^m, and the m_i coefficients are *unambiguous* functions of the parameter $\mathcal{K}$. Their behavior will be considered in what follows.

1. Behavior of $W_i(\mathcal{K}, T)$ and kinetic diagrams $\mathcal{K} - T$

Figs.10,11, and 12 show the plots $W_H = p^{1/4}h_s/h_e, W_L = p^{-1/4}l_s/l_e$, and $W_N = p^{-1/4}N/N_e$ vs $T = \tau/p$ in the $\mathcal{K}$ range from $\mathcal{K} = 10^{-11/2}$ to $\mathcal{K} = 10^{13/2}$ (upper panels), and the corresponding $\mathcal{K} - T$ diagrams of the power-law asymptotic regions (lower panels), obtained by replotting the data of Fig.5 ($J = 10^8$) for $\tau < \tau_r \approx 0.2$ in the corresponding scaling coordinates. It is seen that with the growing $\mathcal{K}$ from $\mathcal{K} \ll 1$, the $W_i(\mathcal{K}, T)$ trajectories initially shift in a self-similar manner in accord with the scaling (45)

$$W_i(\mathcal{K}, T) = \mathcal{K}^{\pm 1/6} v_i(\mathcal{K}^{2/3}T), \quad \mathcal{K} \to 0, \tag{63}$$

(note that for $W_L(\mathcal{K}, T)$ this scaling takes place only at $T \gg 1$ whereas at $T \ll \mathcal{K}^{-2/3}$, according to (28), the scaling $W_L(\mathcal{K}, T) = \sqrt{\mathcal{K}}u(T)$ takes place) and then at $\mathcal{K} \gg 1$ they shift in a self-similar manner at "tails" of $T \ll 1$, in accord with the scaling

$$W_{H,L}(\mathcal{K},T)=\Lambda_s(\mathcal{K}T), \tag{64}$$

$$W_N(\mathcal{K},T)=\mathcal{K}^{-1/2}\Lambda_N(\mathcal{K}T),$$

converging at $\mathcal{K}T\to\infty$ to the universal ($\mathcal{K}$ independent) trajectories (44)

$$W_i(\mathcal{K},T)=w_i(T),\quad \mathcal{K}T\to\infty. \tag{65}$$

Fig.11 clearly demonstrates the evolution of the course of the $W_L(\mathcal{K},T)$ trajectories as a result of competition of two opposite tendencies: (i) growth acceleration of l_s, associated with the reflection of L particles from the boundary $x=0$ and (ii) growth deceleration of l_s, associated with the establishment of quasiequilibrium $J^d\simeq J$, the former being dominant at any $\mathcal{K}$ in the vicinity of $T\approx 1$, the latter in the vicinity of $T\approx T_*=1/\mathcal{K}^{2/3}$ at $\mathcal{K}<1$ and in the vicinity of $T\approx T_q=1/\mathcal{K}$ at $\mathcal{K}>1$, shifting with the growing $\mathcal{K}$ towards $T\to 0$.

The general evolution picture of the power-law asymptotic regions with the growing $\mathcal{K}$ between the limiting regimes (40) and (41) as well as of the $\mathcal{K}$ and T regions, in the confines of which the crossovers between power-law asymptotics fit the scaling laws (63), (64), and (65), are demonstrated by the kinetic $\mathcal{K}-T$ diagrams on the lower panels of Figs. 10,11, and 12. According to Eqs.(56), the given plots yield an exhaustive description of evolution of the h_s, l_s, and N trajectories at the stage of the H particles diffusion into a semi-infinite medium at arbitrary J and p changes. In particular, at $p=$ const. the given plots factually describe the evolution of the h_s, l_s, and N trajectories with the growing density of the flux J up to $T=T_r$, where $T_r\approx 0.2/p$ is the time, begining with which the reflection of H particles from the boundary $x=0$ becomes essential.

2. Scaling of h_s^M

From Eqs.(56) it follows that at $p<1, J\gg J_c$, and $\tau<\tau_r$ the p and J dependences of the h_s^M amplitude and the time τ_M, for which h_s reaches a maximum, should have the scaling form

$$h_s^M=h_e p^{-1/4}M(\mathcal{K}),\quad \tau_M=pT_M(\mathcal{K}). \tag{66}$$

In the limit of small $\mathcal{K}\ll 1$, according to (63),(46), and (49), the scaling $M(\mathcal{K})$ and $T_M(\mathcal{K})$ functions have the asymptotics

$$M(\mathcal{K})=0.7221\mathcal{K}^{1/6},\quad T_M(\mathcal{K})=1.125\mathcal{K}^{-2/3}. \tag{67}$$

In the opposite limit of large $\mathcal{K}\gg 1$ the quantity $M(\mathcal{K})$ reaches its limiting value $M(\mathcal{K}\to\infty)=1$. By differentiating (60), in this limit we find

$$M(\mathcal{K})=1-\left(\frac{\ln 16\mathcal{K}}{8\pi\mathcal{K}}\right)^{1/2}\left(1+\frac{1}{\ln 16\mathcal{K}}\right), \tag{68}$$

$$T_M(\mathcal{K})=\frac{2}{\ln 16\mathcal{K}},$$

whence it follows that $M(\mathcal{K})$ approaches 1 as $1-M\propto\sqrt{\ln\mathcal{K}/\mathcal{K}}$, and a rapid drop of $T_M(\mathcal{K})$ tranforms at $\mathcal{K}\gg 1$ to a slow logarithmic one. In Fig.12 are presented the numerical data of Fig.6 replotted in the scaling coordinates $p^{1/4}h_s^M/h_e$ - $\mathcal{K}$ and τ_M/p-$\mathcal{K}$, respectively. It is seen, that in complete agreement with (62), the points, calculated for different p and J values, fit the scaling functions $M(\mathcal{K})$ and $T_M(\mathcal{K})$ which at small $\mathcal{K}\ll 1$ and large $\mathcal{K}\gg 1$ approach, respectively, asymptotics (67) and (68), shown in dashes.

3. Scaling of ϕ_i^m and m_i

In Figs.13a and b are drawn, respectively, the $|\phi_i|^m$ and T_i^m vs $\mathcal{K}$ dependences derived from the data of Figs.8 and 9, and the analogous data for some other $p<p_s$ and $J>J_{1/4}$ values. The points, calculated in a broad range of p and J, are seen to fit, in accord with (56), the scaling functions $\phi^m(\mathcal{K})$ and $T_i^m(\mathcal{K})$, which in the limit of small $\mathcal{K}\ll 1$ approach the asymptotics (55) (dashed lines)

$$\phi_H^m=0.00108,\quad T_H^m=17.3\mathcal{K}^{-2/3},$$

and in the limit of large $\mathcal{K}\gg 1$ merge and approach the asymptotics (52) (dashed lines)

$$|\phi_i|^m=0.00798,\quad T_i^m=2.51.$$

According to Eqs.(33),(50), and (56), at $p\ll p_s$ and $J\gg J_{1/4}$ in the range of $T_H^m\ll T<T_r$ the $\tilde{\phi}_i(\mathcal{K},T)$ functions ought to asymptotically decay by the law

$$\tilde{\phi}_i(\mathcal{K},T)=m_i(\mathcal{K})/T^{3/4}+\cdots$$

with the coefficients $m_i(\mathcal{K})$, satisfying the condition

$$m_H(\mathcal{K})+m_L(\mathcal{K})=-\beta/4\sqrt{\mathcal{K}}.$$

In Fig.13c are drawn the $\mathcal{K}$ dependences of m_H and $|m_L|$, derived from the data of Figs. 8 and 9, and the analogous data for some other $p\ll p_s$ and $J\gg J_{1/4}$. The points, calculated in a broad range of p and J, are seen to fit the scailing functions $|m_i(\mathcal{K})|$, which in the limit of small $\mathcal{K}\ll 1$ approach the asymptotics (54), (dashed lines)

$$|m_i(\mathcal{K})|=m_i^{(0)}/\sqrt{\mathcal{K}},$$

and in the limit of large $\mathcal{K}\gg 1$ approach the asymptotics (51) (dashed lines)

$$m_H^\infty = -m_L^\infty = 0.023.$$

Figs.(7), (8), (9), and (14) give a complete picture of the crossovers to the universal $(\beta\tau)^{\mp 1/4}$ asymptotics in a broad range of $0 < \mathcal{K} < \infty$, the main features of which can be summarized as follows:

1) With growing $\mathcal{K}$ the ϕ_H^m amplitude grows from the $\mathcal{K}$-independent asymptotics (55) at $\mathcal{K} \approx 10^{-3}$ to the $\mathcal{K}$-independent asymptotics (52) at $\mathcal{K} > 10^5$. The time of its attaining, T_H^m, drops up to $\mathcal{K} \approx 1$ according to the p-independent asymptotics (55), reaching the I-independent asymptotics (52) in the same range of $\mathcal{K} > 10^5$.

2) With growing $\mathcal{K}$ at the critical point $\mathcal{K}_m = 3.0$ the $|\phi_L^m|$ maximum appears, and its amplitude then drops to the $\mathcal{K}$-independent asymptotics (52) at $\mathcal{K} > 10^5$. The time of its attaining, T_L^m, grows and approaches the I-independent asymptotics (52) in the same range of $\mathcal{K} > 10^5$. In the second critical point $\mathcal{K}_c = 7.3$ the $\mathcal{K} > \mathcal{K}_c$ region appears, within which the ϕ_L curves cross zero, changing the sign herewith.

3) Surprisingly, in the narrow vicinity of the critical point $\mathcal{K}_m$ both the time T_H^m and the $|m_L|$ coefficient approach the p-independent asymptotics (55) and (54), respectively, whereas the m_H coefficient approaches the I-independent asymptotics (51): the formers change within the $\mathcal{K} < \mathcal{K}_m$ range as $\mathcal{K}^{-2/3}$ and $\mathcal{K}^{-1/2}$, respectively, the latter remains constant within the $\mathcal{K} > \mathcal{K}_m$ range.

V. LONG-TIME RELAXATION DYNAMICS ($\omega\tau > 1$).

In the light of the results of the previous Section IV, we return, in conclusion, to the analysis of the long-time relaxation dynamics of h_s, l_s, and N, which, according to Section III can be given as

$$h_s = h_e(1 - \sigma_H),$$

$$l_s = l_e(1 - \sigma_L), \tag{69}$$

$$N = N_e(1 - \sigma_N),$$

where $\sigma_H = \tilde{h}_s/h_e, \sigma_L = \tilde{l}_s/l_e$, and $\sigma_N = \tilde{n}/N_e$ at sufficiently large $\omega\tau > 1$ decay by the law

$$\sigma_i = A_i e^{-\omega\tau}(1 + O(e^{-\omega\tau})),$$

and the coefficients A_i are related as

$$A_H = r_s A_L = A_N \sqrt{\omega}\cot\sqrt{\omega}. \tag{70}$$

By preserving in (8) the next-to-leading terms

$$\tilde{h}_s = \mathcal{A}_H \cos(\sqrt{\omega}x)e^{-\omega\tau} + \mathcal{B}_H \cos(\sqrt{2\omega}x)e^{-2\omega\tau} + ...,$$

$$\tilde{l}_s = \mathcal{A}_L \cos(\sqrt{p\omega}x)e^{-\omega\tau} + \mathcal{B}_L \cos(\sqrt{2p\omega}xe^{-2\omega\tau} + ...,$$

from Eq.(7) we easily find

$$\sigma_i = A_i e^{-\omega\tau}(1 + B_i\sigma_N + ...), \tag{71}$$

where the coefficients B_i are defind from the relations

$$B_H = \sqrt{p\omega}\cot\sqrt{p\omega}\cot\sqrt{2\omega}/Q,$$

$$B_L = \sqrt{p\omega}\cot\sqrt{\omega}\cot\sqrt{2p\omega}/Q,$$

$$B_N = \sqrt{p\omega}\cot\sqrt{p\omega}\cot\sqrt{\omega}/\sqrt{2}Q,$$

$$Q = \cot\sqrt{2\omega} + \sqrt{p}\cot\sqrt{2p\omega} - \sqrt{2\omega/J}.$$

By substituting now (69) into (14) and (15) and introducing the designation $\mathcal{D} = \sigma_H\sigma_L$, after having excluded $\hat{\sigma}_H(s)$ and $\hat{\sigma}_N(s)$, we find

$$\hat{\sigma}_L(s) = \frac{\coth\sqrt{s} - (1 - s\hat{\mathcal{D}}(s))\sqrt{p}\coth\sqrt{ps} + \sqrt{s/J}}{s(\coth\sqrt{s} + \sqrt{p}\coth\sqrt{ps} + \sqrt{s/J})} \tag{72}$$

In accord with the results of Section III, the main pole of Eq.(72) ($s = -\omega$) defines the relaxation rate ω as the least positive root of (9) and yields the relaxation "amplitude" A_L in the form

$$A_L = A_{L0}(1 + \tfrac{1}{2}\omega\hat{\mathcal{D}}(-\omega)) \tag{73}$$

where

$$A_{L0} = \frac{4\sqrt{p/\omega}\cot\sqrt{p\omega}}{\sin^{-2}\sqrt{\omega} + p\sin^{-2}\sqrt{p\omega} + 1/\sqrt{J}} \tag{74}$$

and $\hat{\mathcal{D}}(-\omega) = \int_0^\infty \sigma_H\sigma_L e^{\omega\tau}d\tau$. In the diffusion-controlled limit of our concern here, $J \to \infty$, the coefficients B_i change from $B_N = B_L = B_H - 1 = 0.1079...$ at $p \to 0$ to $B_i \to 0$ at $p \to 1$, therefore given that the next after the main root of (9) is an order of magnitude above, we conclude that down to $\tau \sim \omega^{-1}$ the asymptotic behavior of σ_L has the form $\sigma_L = A_L e^{-\omega\tau}(1 + B_L\sigma_N + ...) \simeq A_L e^{-\omega\tau}$. By matching this asymptotics at $\tau = \omega^{-1}$ with that of (32), which for $p \ll 1$ assumes the form $\sigma_L = (1 - \beta\tau^{1/4}(1 + \phi_L)) \simeq 1 - \beta\tau^{1/4}$, in the limit $p \to 0$ we find

$$A_L \simeq e(1 - \beta/\omega^{1/4}) \simeq 0.5 \tag{75}$$

From (73) and (75) it follows that at $p \to 0$ the quantity $\hat{\mathcal{D}}(-\omega) \sim -0.1$ and the difference of A_L from A_{L0} does not exceed 20%. Obviously, with the growing p this difference can only go down, therefore by assuming in the first approximation $A_L \simeq A_{L0}$ and extrapolating the $\mathcal{D} \simeq -A_{L0}^2 e^{-2\omega\tau}$ asymptotics down to $\tau = 0$

$(\hat{\mathcal{D}}(-\omega) \simeq -A_{L0}^2/\omega)$, we finally come to simple expressions

$$A_L = A_H/r_s \sim A_{L0}(1 - \tfrac{1}{2}A_{L0}^2), \tag{76}$$

$$A_N = \frac{4(1 - \frac{1}{2}A_{L0}^2)}{\omega(\sin^{-2}\sqrt{\omega} + p\sin^{-2}\sqrt{p\omega})}, \tag{77}$$

which, according to the numerical data, differ from the exact values by no more than $1 - 2\%$ for any p. Fig.15 gives, as an illustration, the time dependences $|\sigma_H(\tau)|$ and $\sigma_L(\tau)$, calculated numerically at $J = 10^6$ for $p = 10^{-4}, 0.5$ and at $J = 10^8$ for $p = 0.9$ and compared with the results of the calculation from the expressions $\sigma_i = A_i e^{-\omega\tau}$, (9), (76) and (74). The excellent agreement between the numerical and analytical data is evident.

---

[1] For a review see D. ben-Avraham and S. Havlin, *Diffusion and Reactions in Fractals and Disordered Systems* (Cambridge University Press, Cambridge, 2001); E. Kotomin and E. Kuzovkov, *Modern Aspects of Diffusion Controlled Reactions: Cooperative Phenomena in Bimolecular Processes* (Elsevier, Amsterdam, 1996); S. Redner, Scaling theories of diffusion-controlled and ballistically-controlled bimolecular reactions, In:*Nonequilibrium Statistical Mechanics in One Dimension*, Ed. V. Privman (Cambridge University Press, Cambridge, 1997); B. Chopard and M. Droz, *Cellular automata modeling of physical systems*(Cambridge University Press, Cambridge, 1998) and references therein

[2] A.A. Ovchinnikov and Ya.B. Zeldovich, Chem. Phys., **28**, 215, 1978

[3] D. Toussaint and F. Wilczek, J. Chem. Phys., **78**, 2642, 1983

[4] L. Galfi and Z. Racz, Phys. Rev. A, **38**, 3151, 1988

[5] E. Ben-Naim and S. Redner, J. Phys. A, **25**, L575, 1992

[6] S. Cornell and M. Droz, Phys. Rev. Lett., **70**, 3824, 1993

[7] B.M. Shipilevsky, Phys. Rev. Lett., **73**, 201, 1994

[8] B.M. Shipilevsky, J. Phys. A, **30**, L471, 1997

[9] B.M. Shipilevsky, Phys. Rev. Lett., **82**, 4348, 1999

[10] K. Lindenberg, B.J. West and R. Kopelman, Phys. Rev. Lett., **60**, 1777, 1988

[11] D. ben-Avraham and C.R. Doering, Phys. Rev. A, **37**, 5007, 1988

[12] E. Clement, L.M. Sander and R. Kopelman, Phys. Rev. A, **39**, 6455, 1989; **39**, 6466, 1989

FIG. 1. Schematic illustration of the processes of dissociation, desorption, surface migration and diffusion into the bulk in the system $A + B \to 0$ with input of A and B particles. $\ell_A^D = \sqrt{D_A t}$ and $\ell_B^D = \sqrt{D_B t}$ are the diffusion lengths of $A's$ and $B's$ particles, respectively.

FIG. 2. Time dependences $h_s(\tau)/h_e$, calculated numerically at flux densities $J = 1, J_c = 7.250031, 10^2, 10^3$, and 10^4 (bottom to top) for $p = 0.1$.

FIG. 3. Dependence of r_s on $\sqrt{J/J_c}$, calculated from Eq.(5) for $p = 0.1$. Left and right insets demonstrate the specific features of relaxation of surface concentrations at small $J \ll J_c$ and large $J \gg J_c$, respectively.

FIG. 4. Time dependences $h_s(\tau)/h_e$ and $l_s(\tau)/l_e$, calculated numerically at $J = J_c$ (open circles) and $J = 10^3$ (filled circles) for $p = 0.1$.

FIG. 5. (a) Time dependences $h_s(\tau)/h_e, l_s(\tau)/l_e$, and $N(\tau)/N_e$, calculated numerically at $p = 1, 10^{-1}, 10^{-2}, 10^{-3}, 10^{-4}, 10^{-5}, 10^{-6}, 10^{-7}, 10^{-8}$, and 10^{-9} for $J = 10^8$ (the arrows point to the displacement directions of the corresponding trajectories at a change in p from $p = 1$ to $p = 10^{-9}$). The trajectories for $p = 1$ and $p = 10^{-9}$ are given in bold lines; (b), (c) Kinetic $p - \tau$ diagrams of the regions of power-law asymptotics and of steady state (shaded by light gray) for $h_s(\tau)/h_e$ (b) and $l_s(\tau)/l_e$ (c) trajectories calculated numerically at $J = 10^8$ according to condition (48). The characteristic times $\tau_H = 1, \tau_L = p, \tau_q = 1/J\sqrt{p}$, and $\tau_* = 1/J^{2/3}$ are shown in dashed lines. The intersection point of τ_L, τ_q, and τ_* ($\tau_q = \tau_L = \tau_* = 4.64158 \times 10^{-6}$) is marked off by filled circle. The arrow shows the direction of displacement of this point along the τ_L line with the growing flux density J. In Fig.5c the $\beta\tau^{1/4}$ asymptotic region for the $N(\tau)/N_e$ trajectories is distinquished by dark gray.

FIG. 6. Dependences of h_s^M/h_e (a) and τ_M (b) on J, calculated numerically at $p = 10^{-1}, 10^{-2}, 10^{-3}, 10^{-4}, 10^{-5}$, and 10^{-6} (bottom to top and top to bottom in (a) and (b), respectively). Dashed lines show the asymptotics (49).

FIG. 7. Time dependences $\phi_H(\tau)$ (a) and $\phi_L(\tau)$ (b), calculated numerically at $p = 10^{-4}$ for $J = 10^4, 10^5, 10^6, 10^7, 10^8, 10^9, 10^{10}, 10^{11}$, and 10^{12} (right to left).

FIG. 8. Data of Fig.7 for sections $\phi_H > 0$ (a) and $\phi_L < 0$ (b) replotting in double logarithmic scale. Dashed lines show the slope of $-3/4$. Bold lines show the ϕ^0 curve, calculated from Eq.(39).

FIG. 9. Time dependences $\phi_H(\tau)$ (a) and $|\phi_L(\tau)|$ (b) for sections $\phi_H > 0$ and $\phi_L < 0$, respectively, calculated numerically at $J = 10^6$ for $p = 10^{-2n/3}$ with $n = 3, 4, 5, 6, 7, 8$, and 9(right to left). Dashed lines show the slope of $-3/4$. Bold lines show the ϕ^0 curve, calculated from Eq.(39).

FIG. 10. (a) Scaling functions $W_H(\mathcal{K},T)$, derived from the data of Fig5a (p from $p=10^{-1}$ to 10^{-9}, $\tau \le 0.2$) by replotting in scaling coordinates $p^{1/4}h_s/h_e$ vs $T=\tau/p$. (b) Kinetic $\mathcal{K}-T$ diagram of the regions of power-law asymptotics of $W_H(\mathcal{K},T)$, derived from the data of Fig.5b ($\tau \le 0.2$) by replotting in scaling coordinates $\mathcal{K}=p^{3/2}J$ vs $T=\tau/p$. Note the different scale on the T axis in (a) and (b).

FIG. 11. (a) Scaling functions $W_L(\mathcal{K},T)$, derived from the data of Fig5a (p from $p=10^{-1}$ to 10^{-9}, $\tau \le 0.2$) by replotting in scaling coordinates $p^{-1/4}l_s/l_e$ vs $T=\tau/p$. (b) Kinetic $\mathcal{K}-T$ diagram of the regions of power-law asymptotics of $W_L(\mathcal{K},T)$, derived from the data of Fig.5c ($\tau \le 0.2$) by replotting in scaling coordinates $\mathcal{K}=p^{3/2}J$ vs $T=\tau/p$. Note the different scale on the T axis in (a) and (b).

FIG. 12. (a) Scaling functions $W_N(\mathcal{K},T)$, derived from the data of Fig5a (p from $p=10^{-1}$ to 10^{-9}, $\tau \le 0.2$) by replotting in scaling coordinates $p^{-1/4}N/N_e$ vs $T=\tau/p$. (b) Kinetic $\mathcal{K}-T$ diagram of the regions of power-law asymptotics of $W_N(\mathcal{K},T)$, derived from the data of Fig.5c ($\tau \le 0.2$) by replotting in scaling coordinates $\mathcal{K}=p^{3/2}J$ vs $T=\tau/p$. As contrasted from Fig.5c, the regions with $n=1/2$ and $n=1$ are added. Note the different scale on the T axis in (a) and (b).

FIG. 13. (a) Collapse of the dependences of h_s^M/h_e on J from Fig.6a to the scaling function $M(\mathcal{K})$ in scaling coordinates $p^{1/4}h_s^M/h_e$ vs $\mathcal{K}=p^{3/2}J$. Dashed lines show the asymptotics (67) and (68). (b) Collapse of the dependences of τ_M on J from Fig.6b to the scaling function $T_M(\mathcal{K})$ in scaling coordinates τ_M/p vs $\mathcal{K}=p^{3/2}J$. Dashed lines show the asymptotics (67) and (68).

FIG. 14. Collapse of calculated numerically for $p=10^{-4}$ (circles)
and $p=10^{-5}$ (diamonds) dependences $|\phi_i^m(J)|, T_i^m(J)$, and $|m_i(J)|$, and calculated numerically for $J=10^6$ (stars) and $J=10^7$ (squares) dependences $|\phi_i^m(p)|, T_i^m(p)$, and $|m_i(p)|$ to scaling functions $|\phi_i^m(\mathcal{K})|$ (a), $T_i^m(\mathcal{K})$ (b), and $|m_i(\mathcal{K})|$ (c), respectively Filled symbols stand for $i=H$, open symbols stand for $i=L$. In Fig.14a,b filled circle m marks off the point $\mathcal{K}_m=3.0$ with which the $\mathcal{K}\ge\mathcal{K}_m$ region begins where a maximum on the $|\phi_L|$ curves appears. Open circle c marks off the point $\mathcal{K}_c=7.3$ with which the region $\mathcal{K}\ge\mathcal{K}_c$ of crossing of the ϕ_L curve with zero begins. Dashed lines show the asymptotics (52) and (55)(a),(b), and (54) and (51)(c).

FIG. 15. Time dependences $|\sigma_H(\tau)|$ (filled circles) and $\sigma_L(\tau)$ (open circles), calculated numerically at $p=10^{-4}$ and $p=0.5$ for $J=10^6$ and at $p=0.9$ for $J=10^8$ (for the sake of clarity, the data are given beginning with $\tau=10^{-2}$. Straight bold lines show $|\sigma_H(\tau)|$ and $\sigma_L(\tau)$, calculated from the equations $\sigma_i=A_ie^{-\omega\tau}$, (9), (76), and (74).

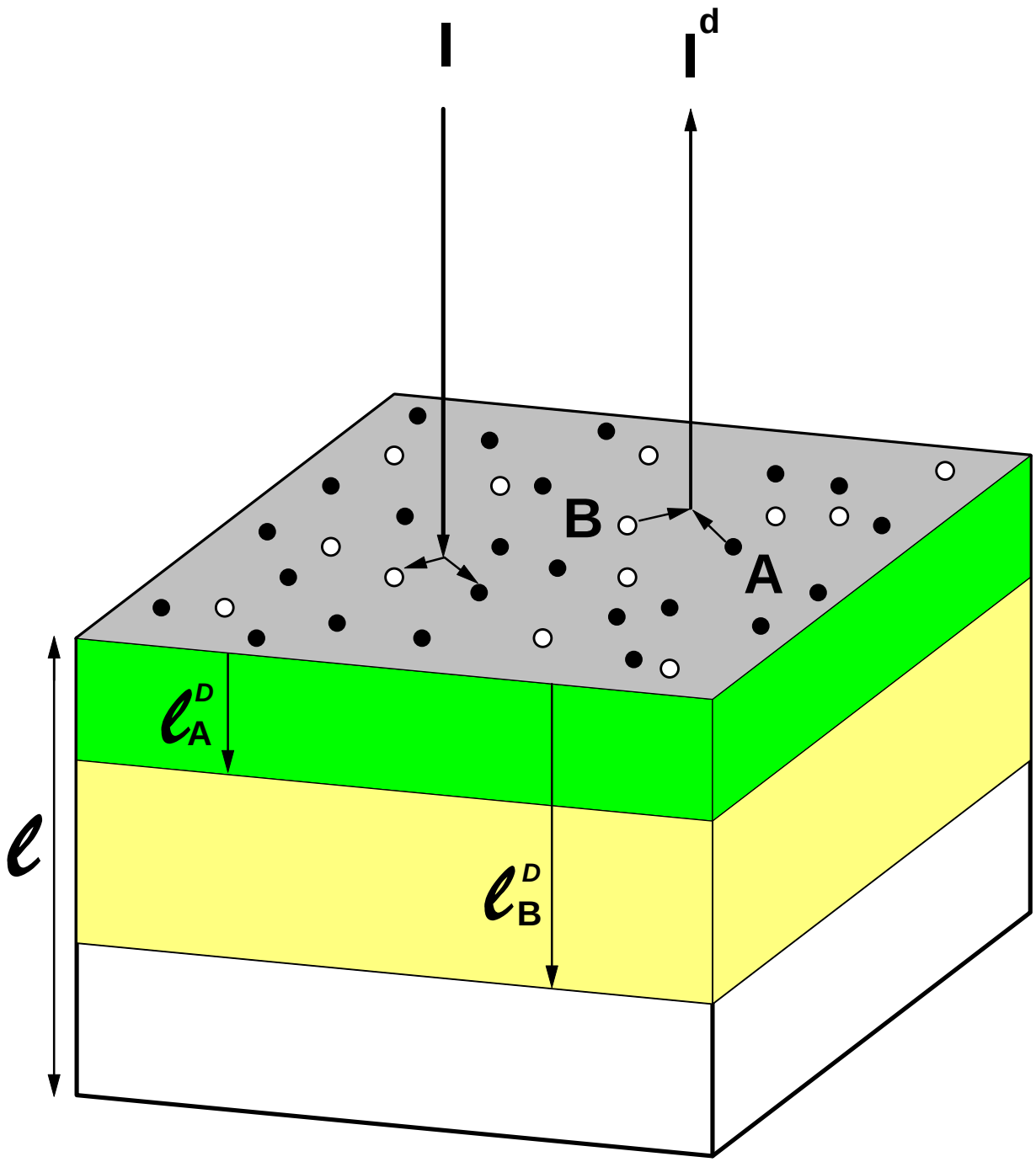
I
I^d
B
A
ℓ
ℓ^D_A
ℓ^D_B

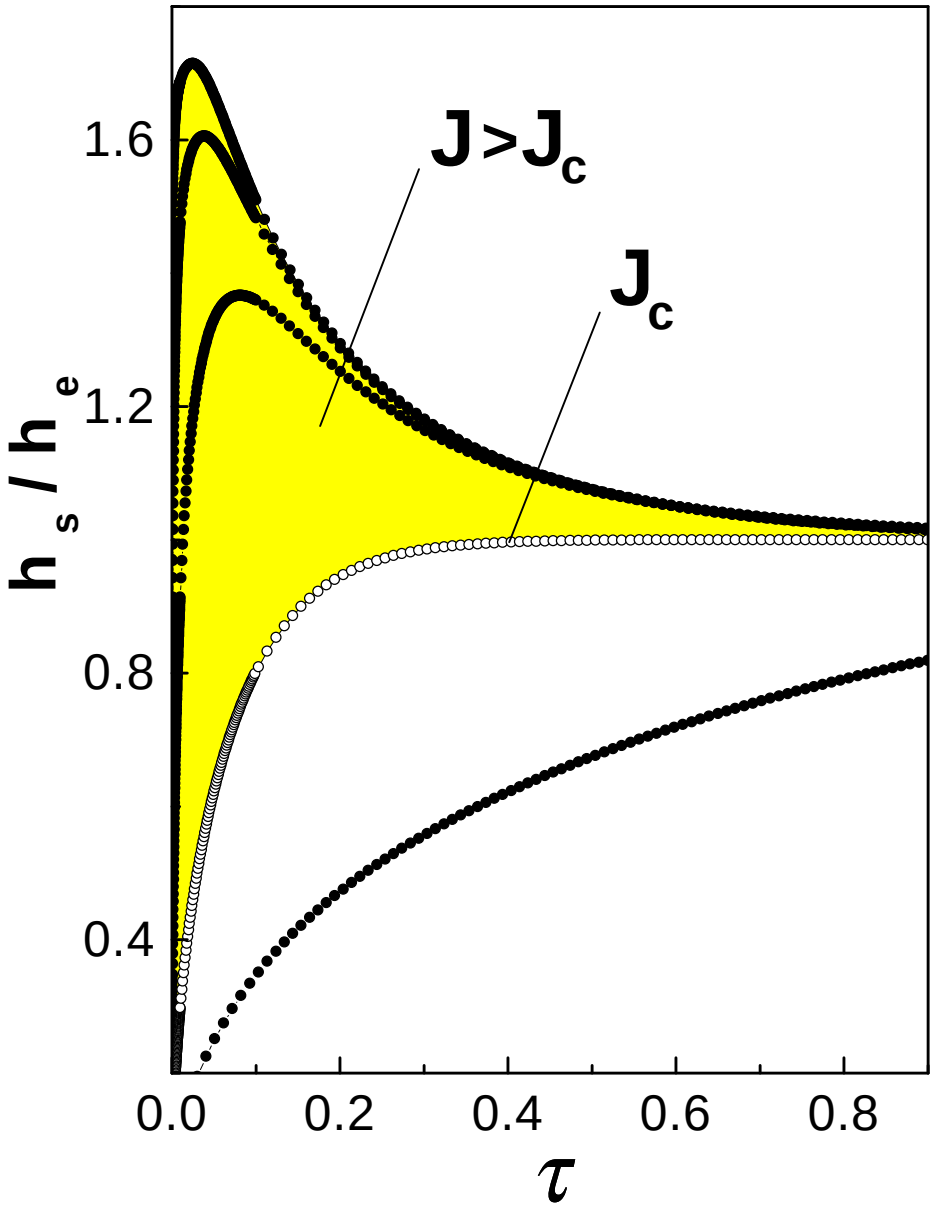
J>Jc
Jc
1.6
1.2
0.8
0.4
h s / h e
0.0
0.2
0.4
0.6
0.8
τ

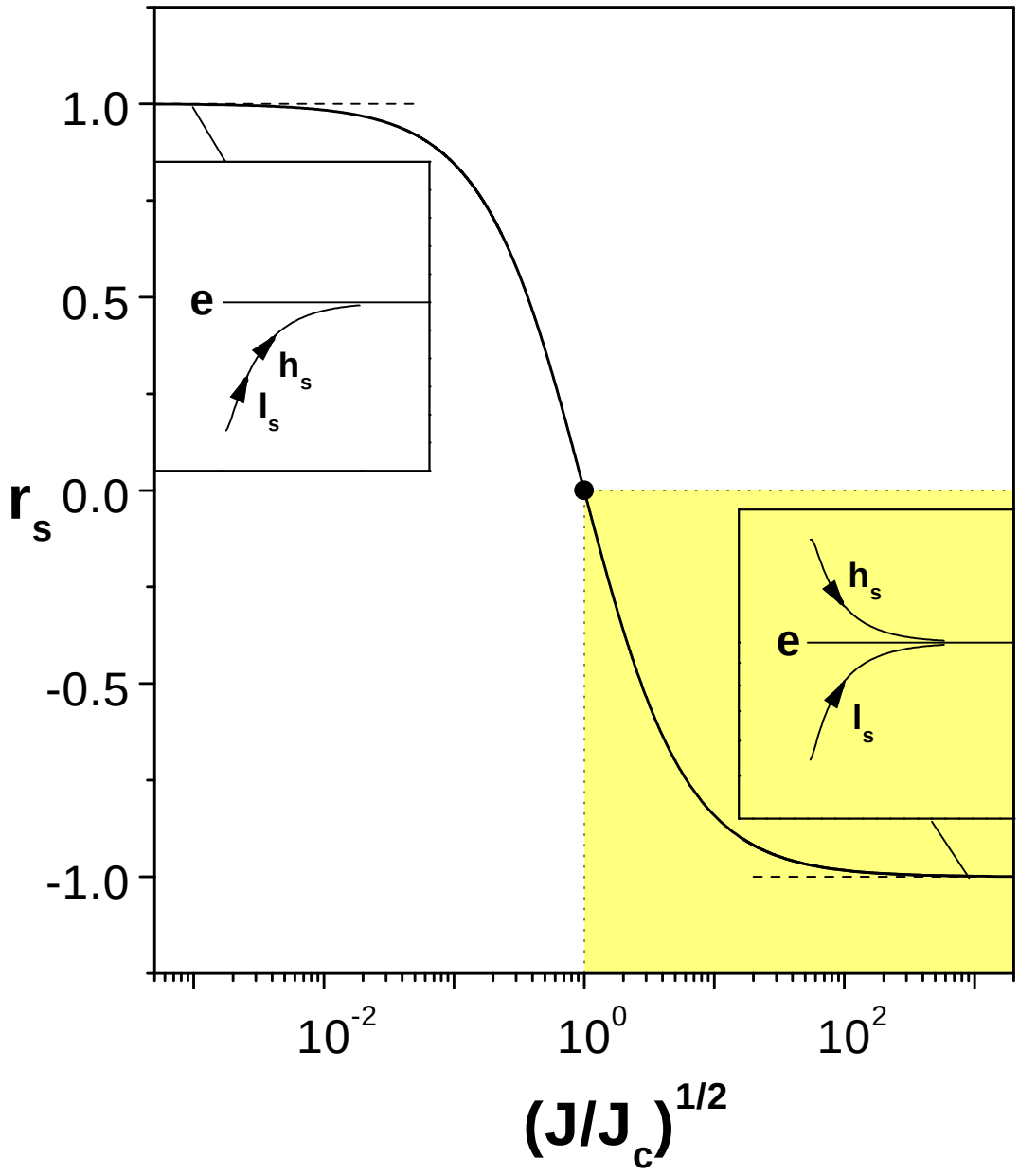
1.0
0.5
0.0
-0.5
-1.0
r_s
e
h_s
l_s
h_s
e
l_s
10^-2
10^0
10^2
(J/J_c)^1/2

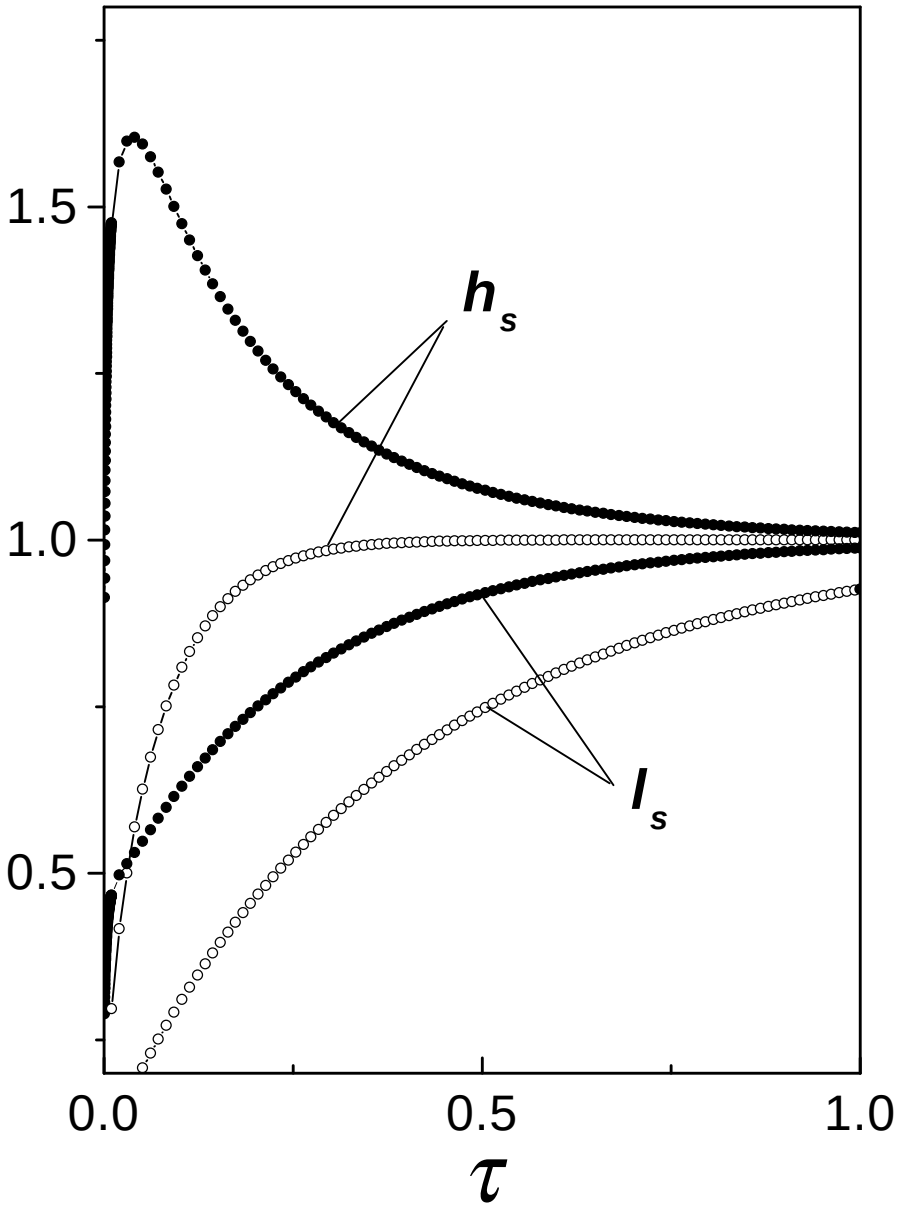
1.5
1.0
0.5
0.0
0.5
1.0
τ
h_s
I_s

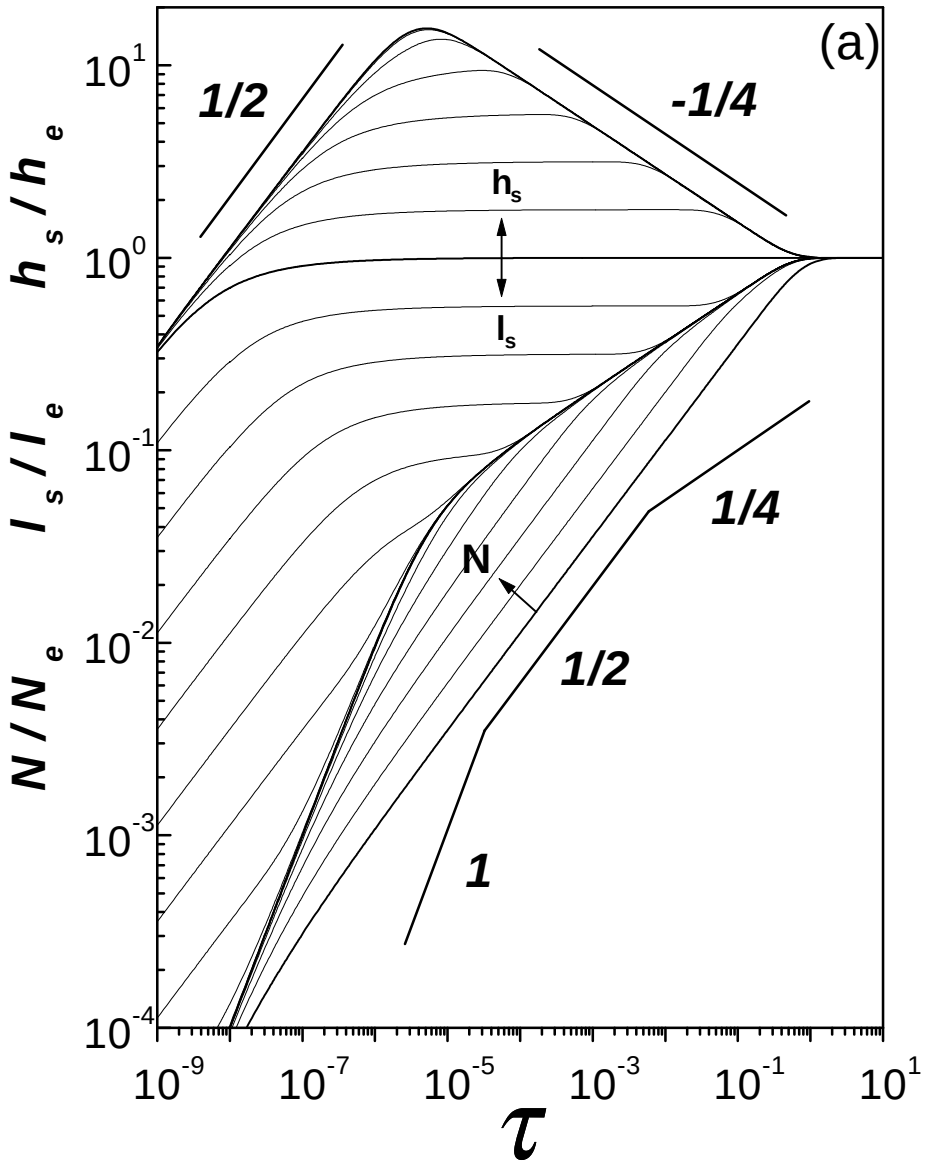
(a)
1/2
-1/4
h_s
l_s
N
1/4
1/2
1
h_s / h_e
l_s / l_e
N / N_e
τ
10^1
10^0
10^-1
10^-2
10^-3
10^-4
10^-9
10^-7
10^-5
10^-3
10^-1
10^1

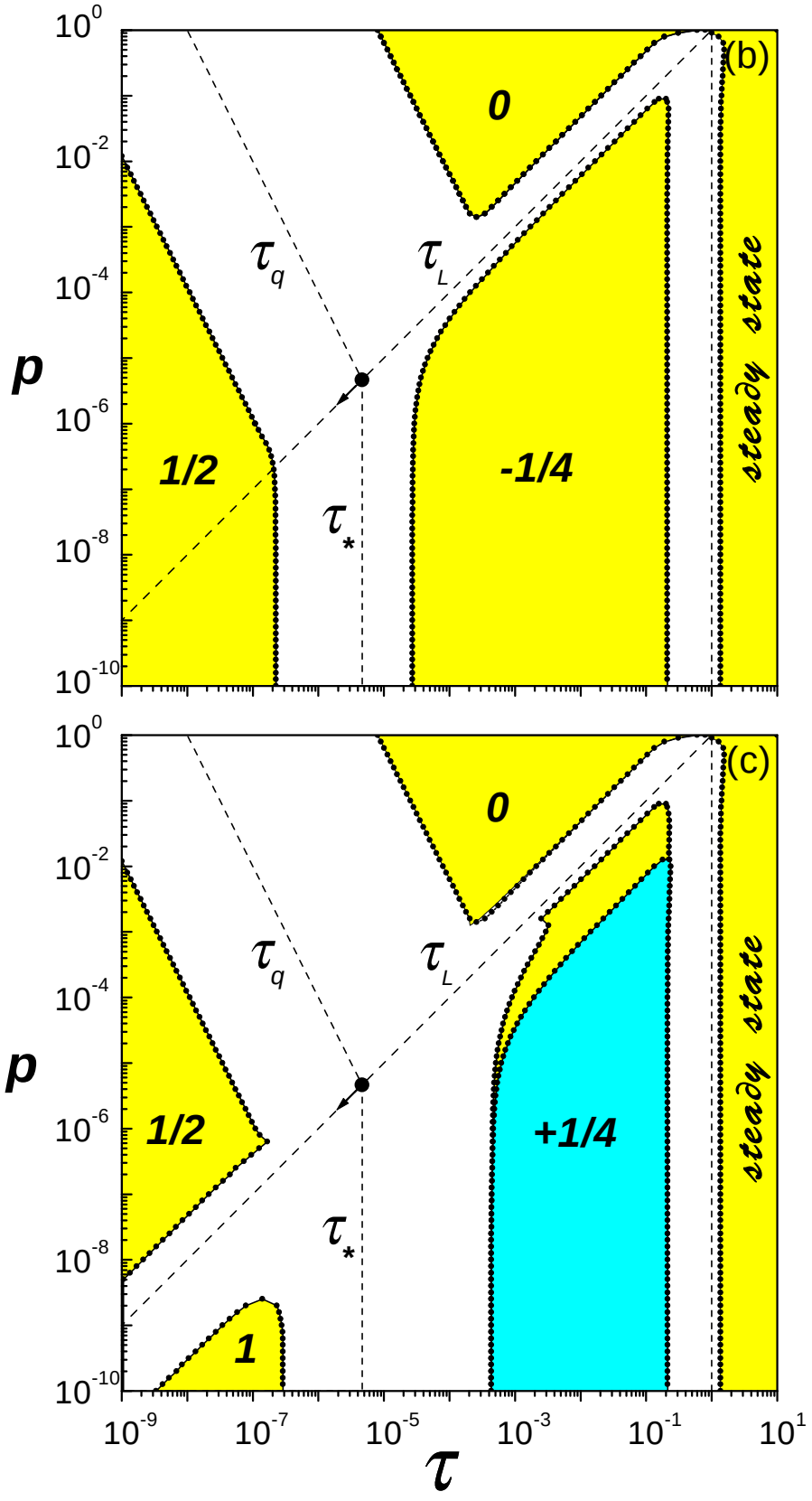
(b)
0
1/2
-1/2
steady state
τ_q
τ_L
τ_*
p
(c)
0
1/2
+1/4
1
steady state
τ_q
τ_L
τ_*
p
τ
10^{0}
10^{-2}
10^{-4}
10^{-6}
10^{-8}
10^{-10}
10^{-9}
10^{-7}
10^{-5}
10^{-3}
10^{-1}
10^{1}

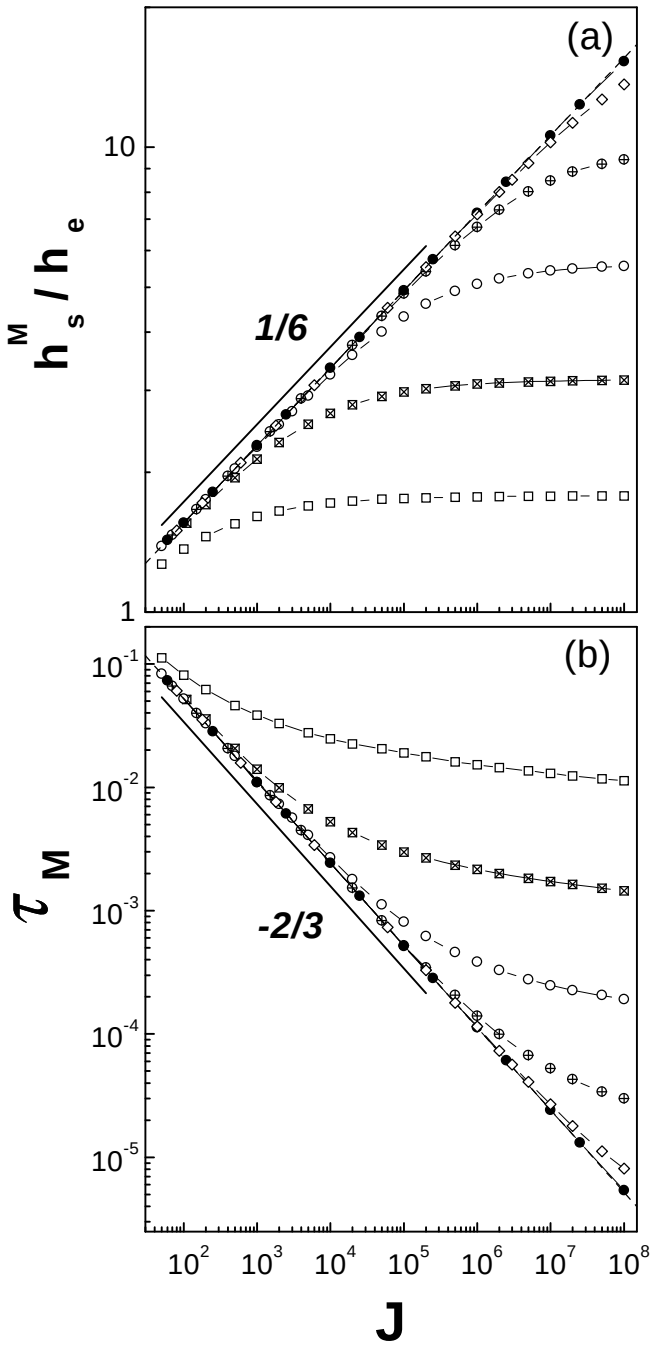
(a)
10
1
h_s^M / h_e
1/6
(b)
10^{-1}
10^{-2}
10^{-3}
10^{-4}
10^{-5}
τ_M
-2/3
10^2 10^3 10^4 10^5 10^6 10^7 10^8
J

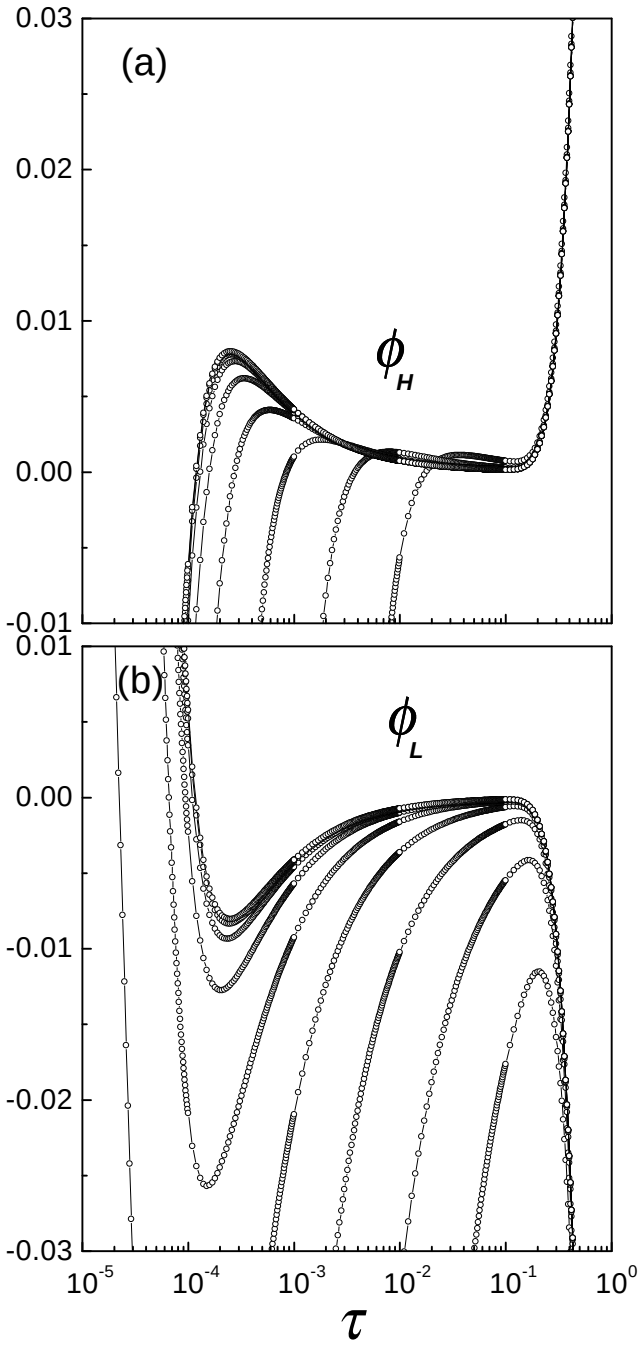
(a)
ϕ_H
(b)
ϕ_L
0.03
0.02
0.01
0.00
-0.01
-0.02
-0.03
10^{-5}
10^{-4}
10^{-3}
10^{-2}
10^{-1}
10^{0}
τ

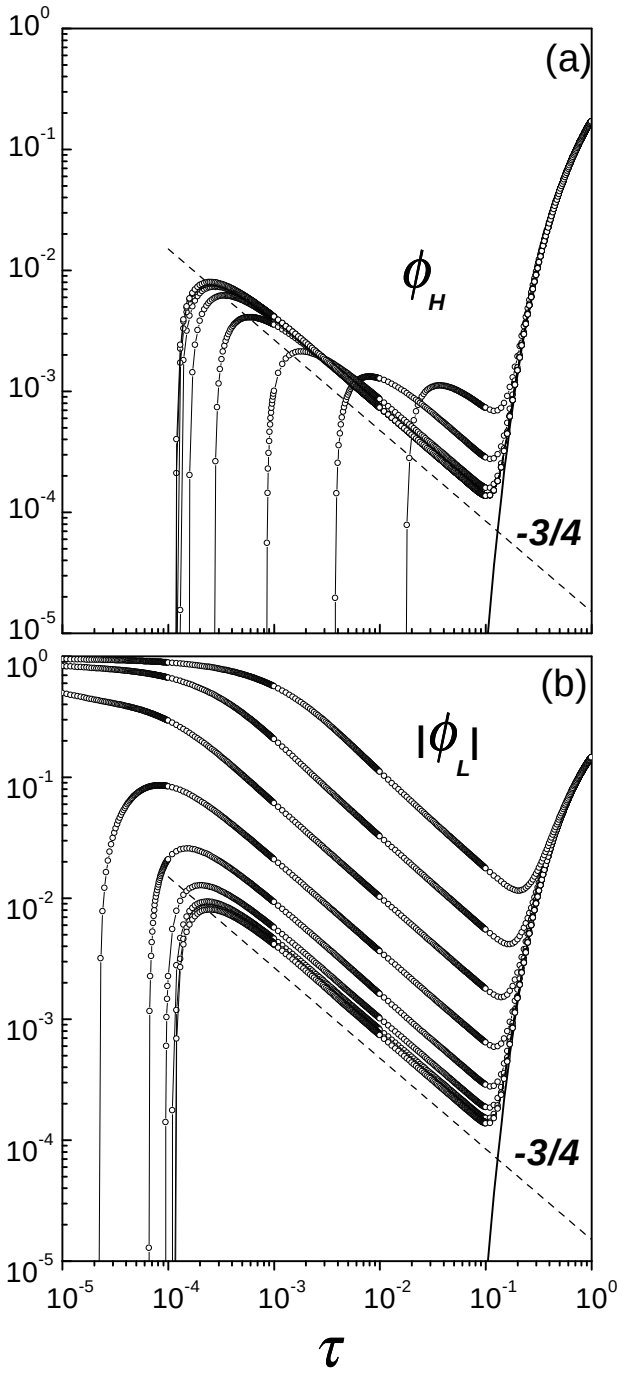
(a)
ϕ_H
-3/4
(b)
$|\phi_L|$
-3/4
10^0
10^{-1}
10^{-2}
10^{-3}
10^{-4}
10^{-5}
τ

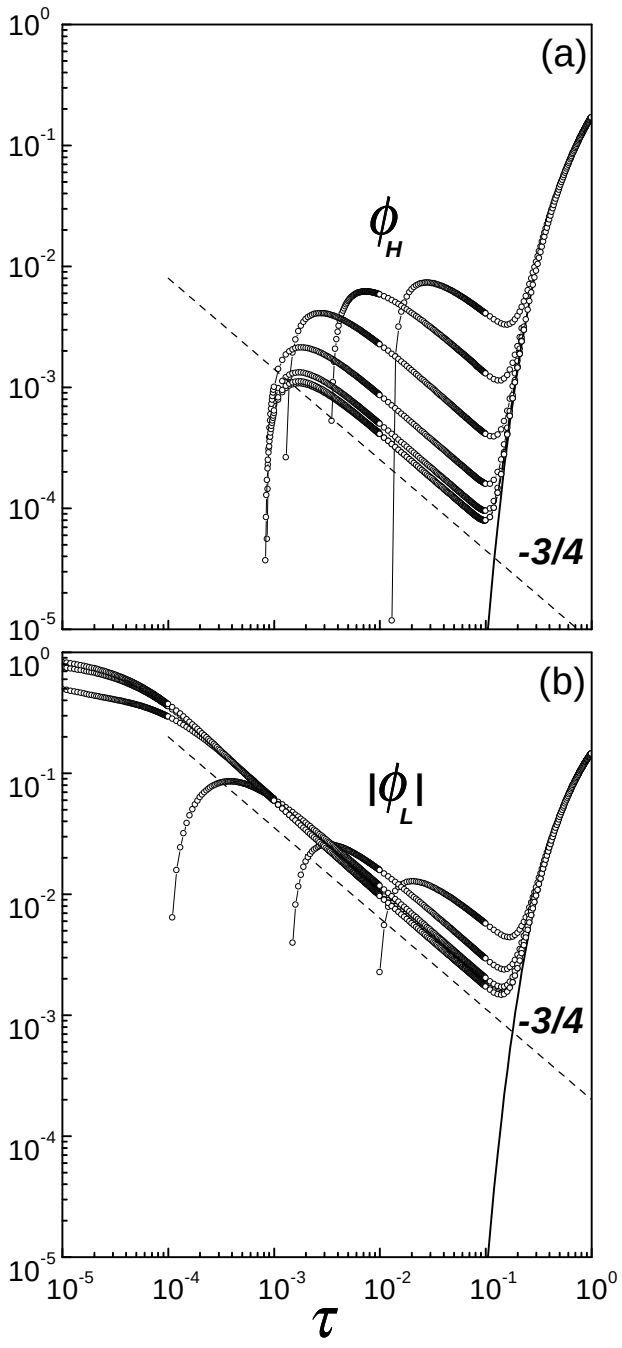
(a)
ϕ_H
-3/4
(b)
$|\phi_L|$
-3/4
10^0
10^{-1}
10^{-2}
10^{-3}
10^{-4}
10^{-5}
τ

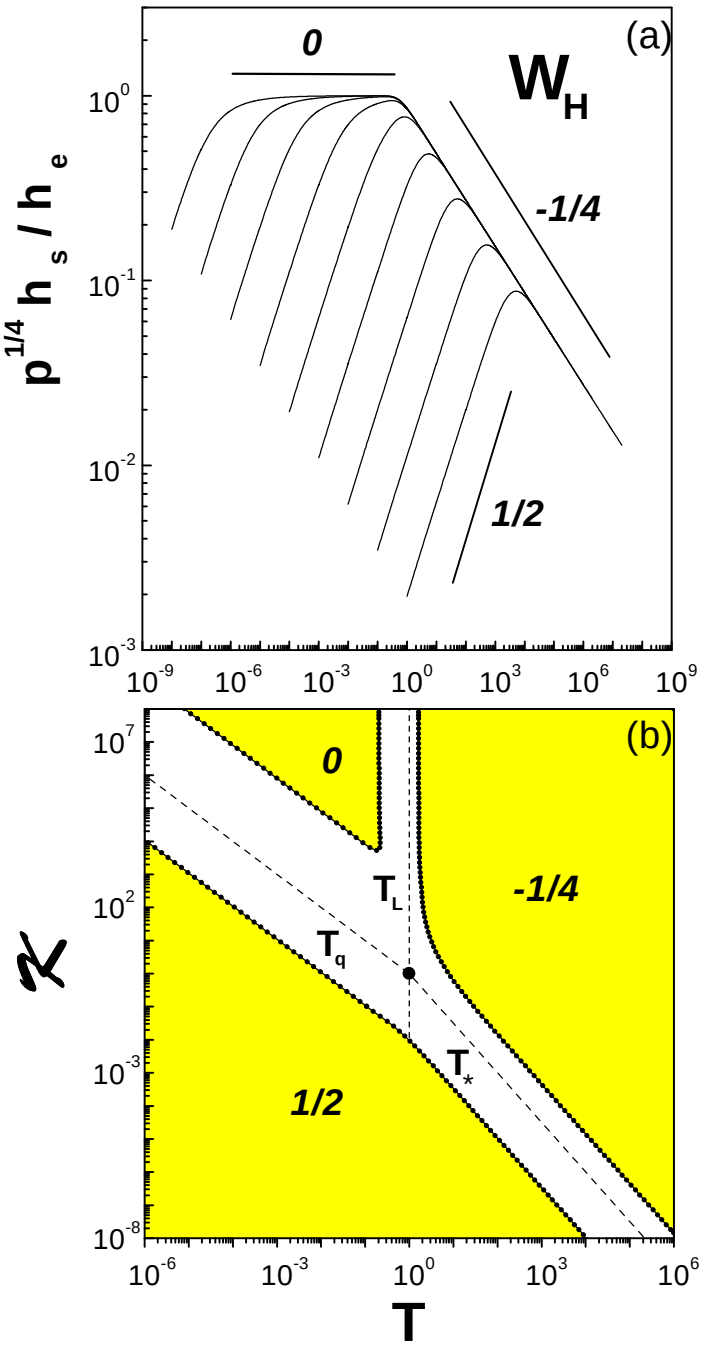
(a)
0
W_H
-1/4
1/2
p^{1/4} h_s / h_e
10^0
10^-1
10^-2
10^-3
10^-9
10^-6
10^-3
10^0
10^3
10^6
10^9
(b)
0
-1/4
1/2
T_L
T_q
T_*
κ
T
10^7
10^2
10^-3
10^-8
10^-6
10^-3
10^0
10^3
10^6

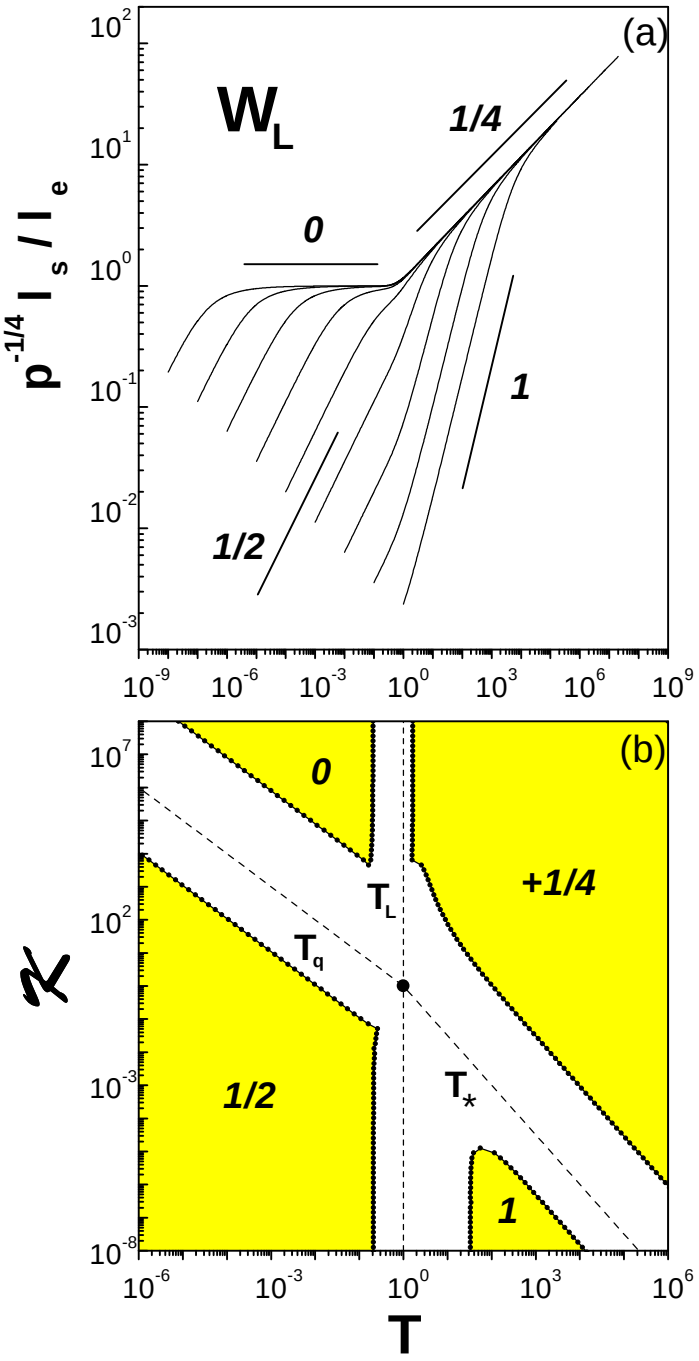
(a)
W_L
1/4
0
1
1/2
$p^{-1/4} I_s / I_e$
10^{2}
10^{1}
10^{0}
10^{-1}
10^{-2}
10^{-3}
10^{-9}
10^{-6}
10^{-3}
10^{0}
10^{3}
10^{6}
10^{9}
(b)
0
+1/4
T_L
T_q
1/2
T_*
1
κ
10^{7}
10^{2}
10^{-3}
10^{-8}
10^{-6}
10^{-3}
10^{0}
10^{3}
10^{6}
T

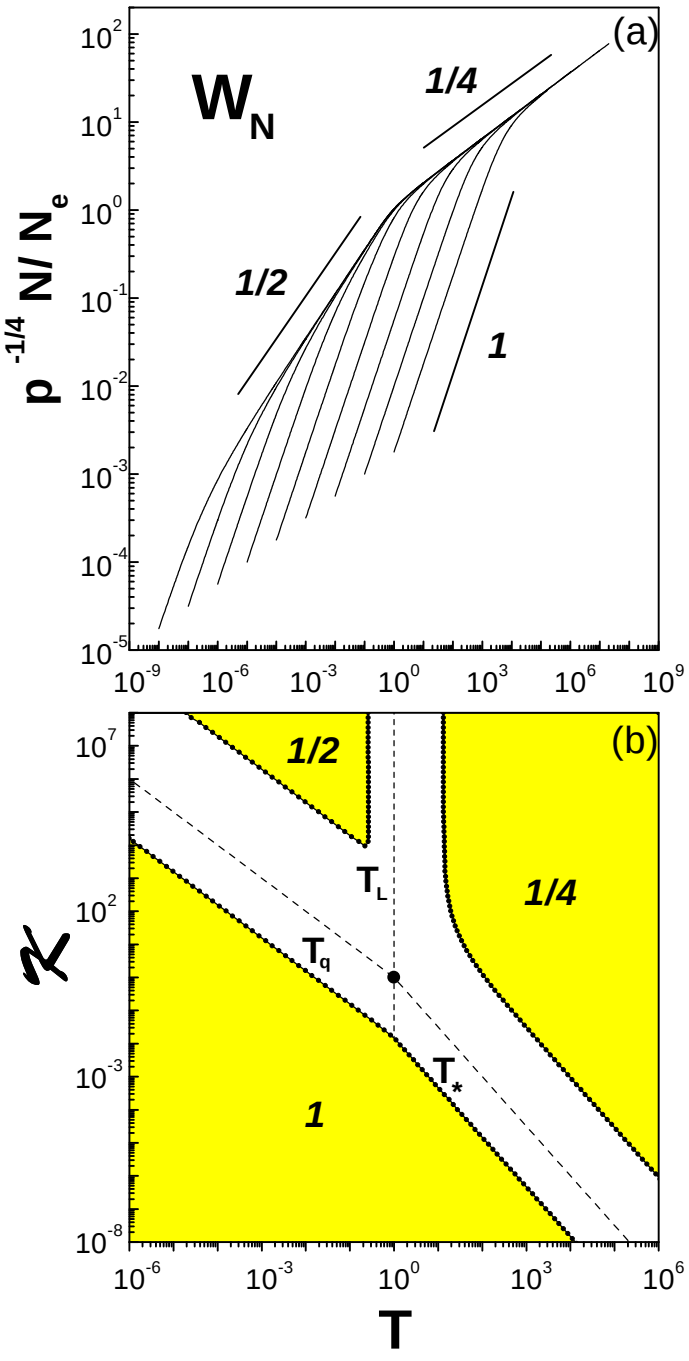
(a)
W_N
1/4
1/2
1
$p^{-1/4} N/ N_e$
10^{2}
10^{1}
10^{0}
10^{-1}
10^{-2}
10^{-3}
10^{-4}
10^{-5}
10^{-9}
10^{-6}
10^{-3}
10^{0}
10^{3}
10^{6}
10^{9}
(b)
1/2
1/4
1
T_L
T_q
T_*
κ
10^{7}
10^{2}
10^{-3}
10^{-8}
10^{-6}
10^{-3}
10^{0}
10^{3}
10^{6}
T

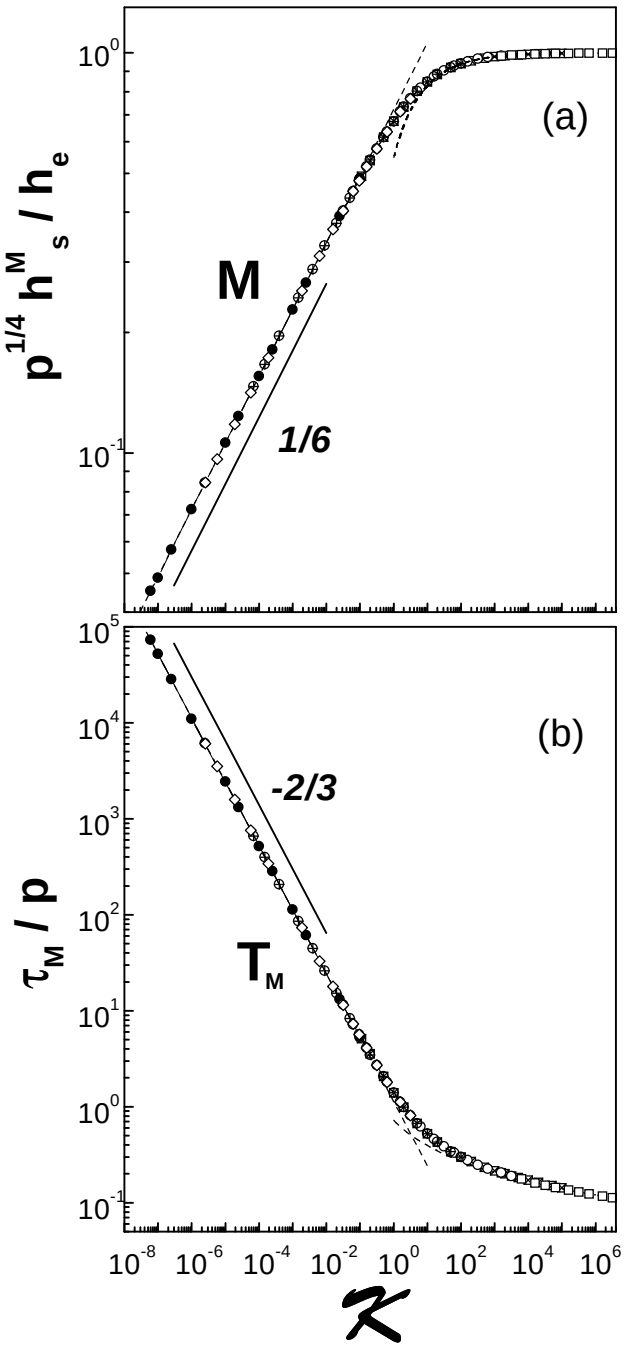
(a)
M
1/6
$p^{1/4} h^M_s / h_e$
(b)
T_M
-2/3
τ_M / p
κ

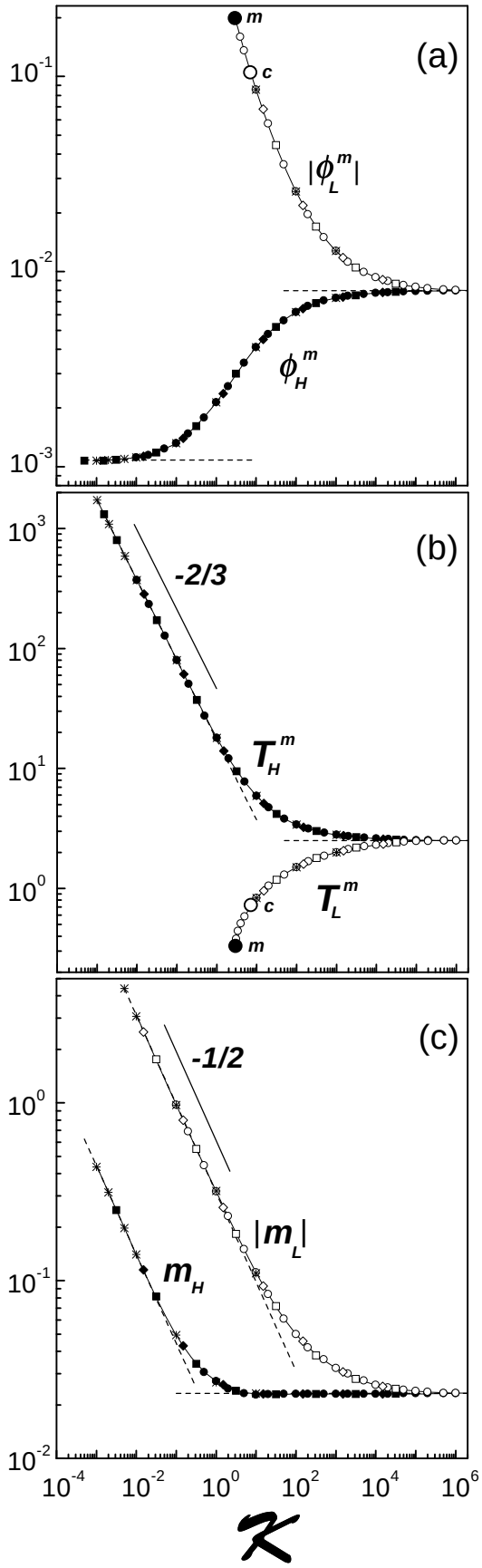
(a)
m
c
$|\phi_L^m|$
ϕ_H^m
10^{-1}
10^{-2}
10^{-3}
(b)
-2/3
T_H^m
T_L^m
c
m
10^3
10^2
10^1
10^0
(c)
-1/2
$|m_L|$
m_H
10^0
10^{-1}
10^{-2}
10^{-4}
10^{-2}
10^0
10^2
10^4
10^6
κ

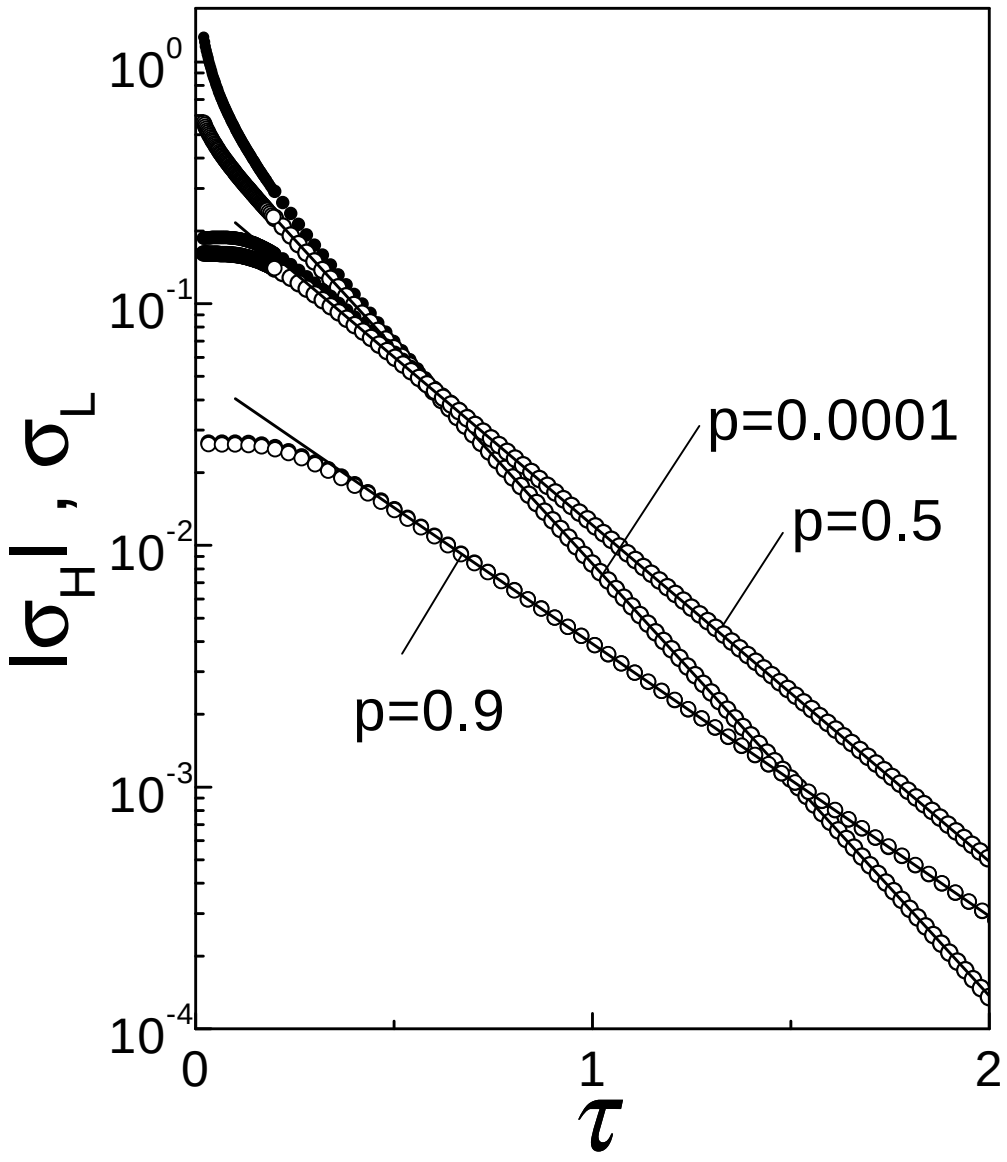
10^0
10^{-1}
10^{-2}
10^{-3}
10^{-4}
$|\sigma_H|$, σ_L
p=0.0001
p=0.5
p=0.9
0
1
2
τ